ABSTRACT

Title of Thesis:	TUBE-LOAD MODEL AS A DIGITAL TWIN FOR ABDOMINAL AORTIC ANEURYSM PATIENTS
	Donghyeon Kim, Master of Science, 2024
Thesis Directed By:	Professor, Jin-Oh Hahn Department of Mechanical Engineering

Abdominal aortic aneurysm (AAA) is a life-threatening condition characterized by the abnormal dilation of the aorta, which can lead to vessel rupture and high mortality rates (>80%). Alarmingly, AAA is often asymptomatic and can remain undetected until it reaches a critical size or ruptures. Current methods for diagnosing and monitoring AAA, such as ultrasound, CT, and MRI, are effective but expensive for regular use and require specialized operators. These limitations hinder the widespread use of imaging-based techniques for regular AAA screening and surveillance. Therefore, creating a need for more accessible, affordable, and convenient tools to detect AAA in its early stages, monitor its progression, and assess treatment efficacy. This thesis explores the potential of tube-load (TL) model to non-invasively monitor AAA progression by analyzing arterial pressure waveforms, which change in response to aneurysm-induced alterations in aortic geometry and mechanical properties. These changes are captured and revealed by the parameters of the TL model.

To evaluate the TL model's capability to monitor AAA, we applied it to carotid and femoral artery tonometry waveforms collected from 79 subjects, including both controls and AAA subjects, as well as a subset of 35 AAA subjects before and after endovascular repair (EVAR) surgery. Our analysis showed that the TL model could fit the waveforms from pre-EVAR AAA subjects as accurately as those from controls and post-EVAR. Moreover, the TL model parameters exhibited physiologically explainable changes consistent with the structural changes of the aorta associated with AAA and its treatment. These findings suggest that the TL model has the potential as a digital twin to enable convenient and cost-effective personalized AAA monitoring.

TUBE-LOAD MODEL AS A DIGITAL TWIN FOR ABDOMINAL AORTIC ANEURYSM PATIENTS

by

Donghyeon Kim

Thesis submitted to the Faculty of the Graduate School of the
University of Maryland, College Park, in partial fulfillment
of the requirements for the degree of
Master of Science
2024

Advisory Committee:
Professor Jin-Oh Hahn, Chair
Professor Jay Lee
Assistant Professor Eleonora Tubaldi

Foreword

Portions of this thesis are taken from and based on the author's own previous work, "Transmission Line Model as a Digital Twin for Abdominal Aortic Aneurysm Patients," originally published as a journal paper by npj Digital Medicine [28].

UNIVERSITY OF MARYLAND

2181 Glenn L. Martin Hall
College Park, MD 20742-3035
TEL: 301-405-2410
http://www.enme.umd.edu

11/7/2024

Re: Previously Published Materials appearing in Thesis or Dissertation

Dean of the Graduate School,

Donghyeon Kim (116484961) has:

☐ NOT INCLUDED any previously published works within their thesis or dissertation.

☒ INCLUDED one or more previously published works within their thesis or dissertation. This letter certifies that the examining committee for the student has determined that the student made a substantial contribution to the previously published work. The inclusion of the previously published work has the approval of the thesis or dissertation advisor and the Graduate Director.

Sincerely,

Peter Sandborn
Director of Graduate Studies
Department of Mechanical Engineering
University of Maryland

Sincerely,

Jin-Oh Hahn
Advisor for Donghyeon Kim

Dedication

To my dear family and friends, for always standing by me through it all.

Acknowledgements

First, I would like to sincerely thank my advisor, Professor Hahn, for his unwavering support and guidance throughout my journey. Despite my many shortcomings, he has always shown compassion, kindness, and understanding. Without his support, I surely would have failed.

Second, I want to thank Dr. Ramakrishna Mukkamala for his support and contributions to my work. Every weekly meeting would end on a positive note thanks to your enthusiasm and positive outlook which helped keep me motivated.

I also want to thank Dr. Jay Lee and Dr. Eleonora Tubaldi for serving on my thesis committee. I'm especially grateful because my defense was held right before Thanksgiving, and they both made time to serve on my committee.

Next, I want to thank the rest of the team that I had the pleasure of meeting and working with: Sina, Zoey, Richard, Weidi, Drew, Yekanth, Jesse, and Parham. Thank you, guys, for all your support and companionship over the years.

Finally, I want to express my deepest gratitude to my family and friends, whose endless love, support, and compassion have carried me through the most challenging moments. Whether I was stressed, overwhelmed, or feeling discouraged, you were always there to cheer me up, keep me grounded, and remind me to persevere. I truly couldn't have made it through this journey without you.

Table of Contents

List of Tables

List of Figures

List of Abbreviations

AAA	Abdominal Aortic Aneurysm
ABI	Ankle-Brachial Index
AI	Artificial Intelligence
AIx	Augmentation Index
BP	Blood Pressure
BSA	Body Surface Area
CON	Control
CT	Computed Tomography
CV	Cardiovascular
CVD	Cardiovascular Disease
DBP	Diastolic Blood Pressure
ECG	Electrocardiogram
EVAR	Endovascular Aneurysm Repair
HR	Heart Rate
IRB	Institutional Review Board
MRI	Magnetic Resonance Imaging
PAD	Peripheral Arterial Disease
PP	Pulse Pressure
PPA	Pulse Pressure Amplification
PTT	Pulse Transit Time
PWV	Pulse Wave Velocity

RC	Reflection Coefficient
RMSE	Root Mean Squared Error
SAAAVE	Screening Abdominal Aortic Aneurysms Very Efficiently
SBP	Systolic Blood Pressure
TL	Tube-Load
2P TL	2-Parameter Tube-Load
3P TL	3-Parameter Tube-Load

Chapter 1: Introduction

1.1 Background

An abdominal aortic aneurysm (AAA) is balloon-like bulge in the aorta, the body's main artery, that gradually expands under blood pressure. As the aneurysm grows, the risk of rupture increases, which can be life-threatening, with a mortality rate exceeding 80% in such cases [1][2]. Although the prevalence of AAA has declined, likely due to a reduction in smoking, its occurrence could increase with society aging [3][4].

AAA can be treated surgically, either through open surgery or endovascular aneurysm repair (EVAR). Both methods have been associated with relatively low mortality rates, as low as 2-3% [1][5]. Despite the low risk of surgery, AAA remains a significant health concern, ranking among the top 15 leading causes of death in the U.S [1]. This raises the critical question: why is AAA so deadly despite the effectiveness of surgery?

1.2 Motivation

AAA's deadliness arises from its asymptomatic nature, earning the condition the reputation of a "silent killer." The asymptomatic progression makes regular screening and monitoring essential, yet screening and surveillance techniques that are both convenient and affordable are not readily available today.

While accurate AAA diagnosis is possible using imaging-based techniques, like ultrasound, CT, and MRI, these methods are often underutilized for screening

and surveillance due to their relatively high cost and inconvenience. Even ultrasound, despite its high sensitivity (94-100%) and specificity (98-100%), safety, and relative affordability, faces similar challenges [6]. Physical examination via palpation is another option, but this requires a skilled examiner and can be unreliable when the AAA is small or the patient is not thin, with a sensitivity of 39-68% at a specificity level of 75%. As such, novel methods to support more frequent and convenient AAA monitoring at a low cost can transform the field and help to save lives [5]-[7].

In the U.S., the "Screening Abdominal Aortic Aneurysms Very Efficiently" (SAAAVE) Act offers a one-time AAA screening for qualifying individuals. However, despite these efforts, it has been shown that a one-time screening has not been effective in preventing AAA rupture which is the primary cause of death for those with the condition [8][9]. Additionally, it is important to note that eligibility under the SAAAVE Act is limited to individuals with a family history of AAA or men with a history of smoking, leaving many others without access to this option.

The underutilization of imaging-based techniques, especially ultrasound, despite their proven effectiveness and the existence of legislation like the SAAAVE Act, highlights a significant gap in regular screening and surveillance techniques for AAA. Even with policies in place to encourage screening, the absence of affordable and accessible screening and monitoring solutions leaves many at risk, underscoring the need for improved tools to screen and monitor AAA.

1.3 Objectives

This thesis aims to begin addressing the significant gaps in AAA screening and surveillance techniques by proposing a physics-based modeling approach to non-invasively monitor arterial hemodynamics. This may provide valuable insights into the progression of AAA in an individual. The proposed model may be able to complement existing biomarkers and risk factors that are commonly used today and help support the development of methods to more convenient and affordable diagnosis and monitoring solutions. It has the potential to serve as a digital twin by allowing physicians to measure, track, and update parameters personalized to an individual patient that can provide insights into their health. This will help the efforts to detect AAA early, monitor its progression, and assess treatment efficacy improving overall patient outcomes.

1.4 Thesis Outline

Chapter 1 will introduce the problem space and explain the current gaps.

Chapter 2 provides a brief overview of hemodynamic and cardiovascular health monitoring.

Chapter 3 provides details of the TL model necessary to accurately understand and interpret the results, and how they relate to the pathology of AAA.

Chapter 4 shows the experimental dataset used in the study and the methods used to fit the model to the data and estimate the parameters.

Chapter 5 presents the results of the TL model and discusses its efficacy as a digital twin for diagnosing and monitoring AAA.

Chapter 6 summarizes the contributions and provides suggestions for future work to be conducted.

Chapter 2: Literature Review

2.1 Hemodynamics and Cardiovascular Health

Cardiovascular diseases (CVD) are ranked consistently as the leading cause of death in the U.S., exceeding even the death toll of cancer. A significant body of evidence suggests that cardiovascular disease develops over a person's lifetime, starting with the emergence of risk factors contributing to the development of subclinical atherosclerosis (i.e., asymptomatic plaque buildup in the arteries) [10][11]. To better monitor patient health, physicians utilize "biomarkers" to help identify vulnerable patients who are at risk for CVD [12]. Biomarkers are defined as an objectively measured quantity that indicates normal biological or pathogenic processes, or pharmacological responses to a therapeutic intervention [13]. For example, blood pressure is a commonly used biomarker, as hypertension is a major risk factor for cardiovascular diseases and the leading single contributor to all-cause mortality worldwide [14].

Particularly, central blood pressure (i.e., blood pressure measured closest to the heart) is regarded as more informative because blood pressure and flow waveforms become increasingly distorted as they travel further from the heart (see figure 1). Notably, pulse pressure (PP)—defined as the difference between systolic and diastolic pressures—tends to amplify as the BP waveform propagates. The degree of this amplification can be influenced by factors such as blood pressure and age-related changes in pulse wave velocity (PWV), as well as variations in peripheral resistance that affect wave reflection characteristics. Therefore, central blood pressure

is the measure that most directly reflects cardiac performance [15]. Other biomarkers, like carotid-femoral PWV and pulse pressure amplification (PPA), are also used to assess the risk of CVD. These biomarkers will be further discussed in chapter 3 within the context of the TL model.

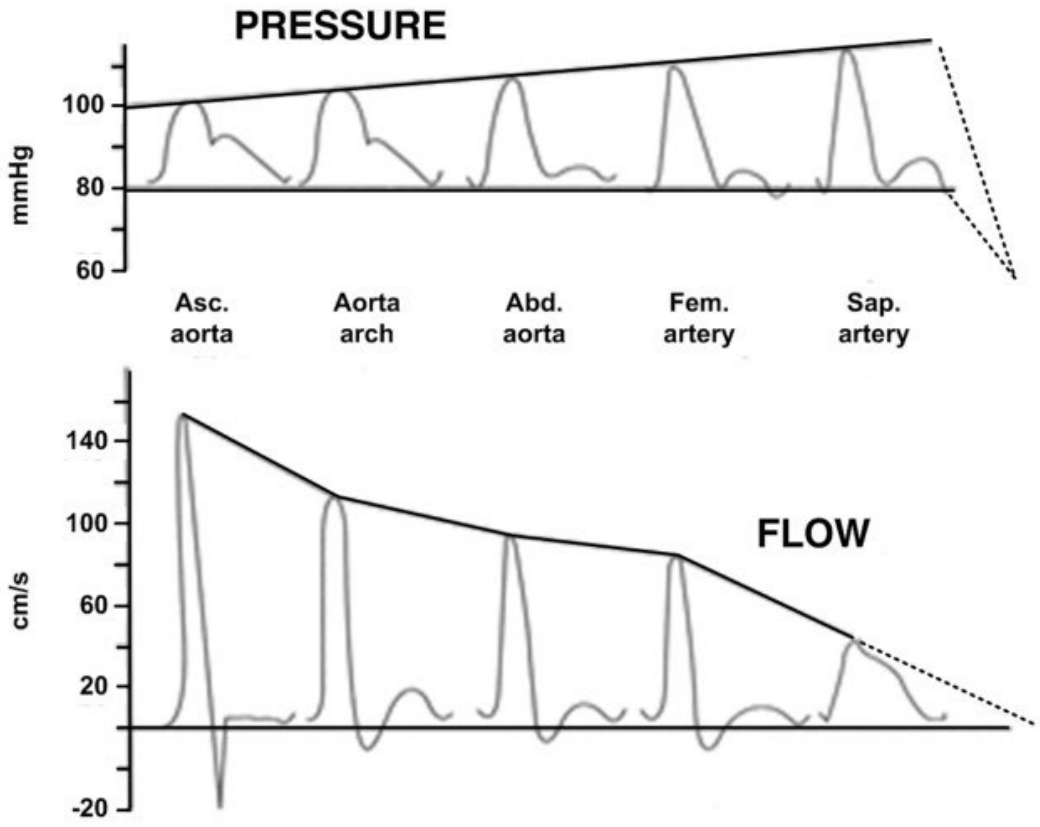

Figure 2-1. Blood pressure and flow waveforms with increasing distance from the heart [16].

Furthermore, central BP is a major determinant of degenerative changes that occur in aging, hypertension, and other cardiovascular diseases [16][17]. This makes central BP valuable in clinical practice, but its usefulness is limited by the difficulty of accurately measuring central BP without invasive methods, like directly inserting a catheter into the aorta. Typically, carotid tonometry measurement is used as a surrogate for central BP since it avoids direct catheterization of the aorta. This

technique is performed by applying an appropriate amount of pressure on an artery close to the skin surface to detect blood pressure. However, it utilizes costly probes and requires a trained operator to apply the "correct" amount of pressure to accurately measure the blood pressure [18][19]. However, it is still a useful tool that can be used to gather valuable insights about a patient's cardiovascular health.

Aside from tonometry, several other methods to non-invasively measure blood pressure have been developed, particularly for the peripheral arteries, including auscultation, oscillometry, and volume clamping. While these methods allow for convenient ways to measure peripheral blood pressure, it does not change the fact that peripheral blood pressure waveforms are subject to distortion as they travel away from the heart. So, improving and/or developing methods to accurately measure or monitor central BP non-invasively will help to save lives. Similarly, monitoring AAA could be done via monitoring central BP, as the mechanical and geometric properties of the aorta change in the presence of AAA. This alters blood pressure wave propagation and reflection characteristics which could potentially contain information that reveals whether a patient has AAA. However, we currently lack ultra-convenient means to obtain such biomarkers of AAA to allow for diagnosis, monitoring, and assessment of treatment efficacy [20].

2.2 Digital Twins in Healthcare

A key challenge in healthcare is providing individualized insights into a patient's health. Personalized healthcare involves accounting for each patient's unique medical history, genetic background, and lifestyle which may affect their response to treatment. Additionally, this requires a substantial amount of data,

advanced analytical tools, and close patient monitoring. Integrating and analyzing this vast amount of information to offer tailored recommendations remains a complex task. However, advancements in artificial intelligence (AI) and big data have revolutionized how industries operate by introducing advanced data-driven decision-making systems leveraging powerful machine learning models, dubbed as "Industry 4.0," bringing us one step closer to personalized healthcare. Digital twins, which create dynamic digital replicas of physical entities, have the potential to transform healthcare significantly by enabling predictive analytics of treatment outcomes, early detection of risk factors, and helping to develop preventative interventions based on personalized digital models that consider individual medical history.

Applications of digital twins in healthcare are not limited to personalized medicine. By virtue of their parametric nature, digital twins can simulate a wide range of virtual patients which is invaluable in assessing how a medical device, drug, procedure, or treatment may perform on a patient. Physiology can vary significantly between individuals so extensive testing is necessary to confidently determine the efficacy and safety of medical interventions. Digital twins enable researchers and physicians to explore diverse patient profiles and conditions without the ethical and logistical challenges associated with obtaining data from real humans. In medical research and drug development, digital twins can be used to accelerate drug discovery and biomarker identification by simulating physiological effects to test drug efficacy and side effects. They can also be used in medical device design by giving engineers a platform to test and refine devices before clinical trials. In surgical planning, digital

twins can be used to simulate complex procedures, providing additional training and helping to improve patient safety and outcomes [21].

Likewise, in the context of monitoring AAA, digital twins hold remarkable potential. AAAs are often asymptomatic, which poses significant challenges for early detection and treatment. Early detection is crucial to managing AAA because, if left untreated, the aneurysm can rupture, which has a mortality rate exceeding 80%. Not only that, more than 60% of these deaths occur before the patient can even reach the hospital, highlighting the urgency of identifying AAA before they reach a critical size [21]. However, many AAAs are found incidentally while screening for other purposes [1], meaning that by the time an AAA is diagnosed, it may have reached a size that is at significantly increased risk of rupture. Digital twins offer a promising solution to enhance the early detection and monitoring of AAA by creating a personalized, virtual representation of a patient's vascular system.

Chapter 3: Arterial Hemodynamics Modeling

3.1 Introduction

Arterial hemodynamic models have existed for a long time and can be divided into two categories: lumped-parameter models and distributed-parameter models, each with their unique advantages and disadvantages. One of the most prevalent lumped-parameter models is the "Windkessel" model, which is characterized by a capacitor and a resistor in parallel. The capacitor represents the arterial compliance while the resistor represents the total peripheral resistance. Lumped-parameter models, such as the Windkessel model, are characterized by a small number of parameters making them useful for parameter estimation purposes from clinically available signals. However, a critical drawback of the Windkessel model is that it assumes infinite pulse wave velocity which prevents them from replicating the wave propagation and reflection phenomena that is critical to accurately representing arterial hemodynamics [16].

In contrast, distributed-parameter models incorporate finite pulse wave velocity, allowing them to replicate the wave propagation and reflection phenomena. Based on the simplified Navier-Stokes equation, distributed-parameter models account for the geometrical and mechanical properties of the arteries explicitly as model parameters, including branching, elastic and geometric tapering, and arterial terminations. These models can offer a much more accurate representation of the arterial tree but cannot be readily applied in parameter estimation applications due to

their heavy computational load and inability to obtain unique parameter estimates stemming from the excessive number of parameters.

To achieve the computational efficiency of the Windkessel model while accurately capturing key aspects of wave propagation and reflection, a category of distributed-parameter models known as tube-load (TL) models has been developed. At their core, TL models are formed by a tube, which represents the artery (i.e., the wave propagation path), that is terminated by a load that signifies the wave reflection point. The pressure and flow waves move forward along the tube without distortion and are proportional to each other. When these waves reach the load, they are reflected backward due to the impedance mismatch between the tube's characteristic impedance and the load. The reflected waves travel in the backward direction and, like the forward waves, propagate without distortion and are proportional to each other. As a result, the arterial pressure and flow waves at any given point along the tube are the sum of the forward and backward traveling waves, adjusted by the time taken to reach the point of interest.

Due to their mathematical tractability and ability to replicate wave propagation and reflection, TL models have become an attractive platform for improving non-invasive monitoring of arterial hemodynamics. As such, a wide variety of TL model variations have been developed and investigated: elastically and/or geometrically tapered tubes, lossy or lossless tubes, and parametric or non-parametric loads [16]. These modifications are designed to better represent the actual behavior of arteries in the body, moving beyond the simplification of treating them as uniform, lossless tubes.

3.2 Uniform Lossless Tube-Load Model

3.2.1 Background

Interestingly, it was discovered that the simplest of these models: the uniform lossless tube terminated by a parametric load (hereafter simply called the tube-load model) is almost as accurate as the most complicated of the models [16]. The tube-load model is quite attractive for its ability to fit arterial pressure and flow waveforms well despite being characterized by only a few parameters. It combines the simplicity of the Windkessel model through its parametric load while retaining the assumption of finite pulse wave velocity of distributed-parameter models to accurately replicate blood pressure wave propagation and reflection.

Great efforts have been made to validate the tube-load model (and its variations) in animal studies [22]. Its ability to replicate inlet-outlet blood pressure (BP) relationship in normal large arteries, including the aorta, in humans has also been established [22]-[24]. However, it has yet to be confirmed whether TL models can replicate BP propagation and reflection characteristics in aneurysmal arteries.

On one hand, existing TL models generally assume that the aortic cross-sectional area remains constant or decreases monotonically. This assumption may hinder their ability to accurately represent an aneurysmal aorta, which features a sudden change in aortic cross-section along the artery. On the other hand, TL models are phenomenological. As such, they may still be capable of effectively replicating the characteristics of blood pressure wave propagation and reflection within an aneurysmal aorta by appropriately adjusting its parameters.

3.2.2 Formulation

The general relationship between the carotid and femoral (i.e., proximal and distal) BP waveforms is given in the Laplace domain as follows:

$$P_C(s) = \frac{e^{\tau s} + \Gamma(s)e^{-\tau s}}{1 + \Gamma(s)} P_F(s) \tag{3.1}$$

where P_C and P_F are the carotid and femoral artery blood pressure waveforms, respectively. Γ is the reflection coefficient (RC) at the tube-load interface, and τ is the pulse transit time (PTT). The pulse transit time, τ, is given by:

$$\tau = d\sqrt{l_l c_l} = d\sqrt{\frac{2\rho r_T}{Eh}} \tag{3.2}$$

where d is the distance between the proximal and distal aortic measurements (which may be approximately proportional to height), $l_l = \frac{\rho}{A_T}$ is aortic inertance per unit length, $c_l = \frac{2A_T r_T}{Eh}$ is the aortic capacitance per unit length, ρ is blood density, $A_T = \pi r_T^2$ is aortic cross-sectional area, r_T is aortic radius, E is aortic stiffness (i.e., aortic elastic modulus), and h is aortic wall thickness. The reflection coefficient, $\Gamma(s)$, is given by:

$$\Gamma(s) = \frac{Z_L(s) - Z_c}{Z_L(s) + Z_c} \tag{3.3}$$

where Z_c is characteristic impedance of the tube and $Z_L(s)$ is the impedance of the frequency-dependent load. Since the tube is characterized by constant inertance, l_l, and compliance, c_l, per unit length, the tube has constant characteristic impedance $Z_C = \sqrt{l_l/c_l}$. The structure of $Z_L(s)$ depends on the structure of the load. We

considered two types of terminal load structures: (i) a single terminal resistor and (ii) a Windkessel load. In the case of a single resistor as the terminal load:

$$Z_L = Z_c + R_L \tag{3.4}$$

and in the case of a Windkessel load as the terminal load:

$$Z_L(s) = Z_c + \frac{R_L}{1 + sR_L C_L} \tag{3.5}$$

where R_L is the peripheral resistance exerted by the arterioles, and C_L is the arterial compliance of the distal artery. This produces two versions of the TL model: (i) the 2-parameter (2P) TL model corresponding to the single resistor as the terminal load structure, and (ii) the 3-parameter (3P) TL model corresponding to the Windkessel load as the terminal load structure. In the case of the 2P TL model, the reflection coefficient reduces to a constant:

$$\Gamma = \frac{R_L}{2Z_c + R_L} \tag{3.6}$$

while in the case of the 3P TL model, the reflection coefficient can be characterized by two lumped parameters:

$$\Gamma(s) = \frac{R_L}{2Z_c R_L C_L s + 2Z_c + R_L} = \frac{\eta_2}{s + \eta_1} \tag{3.7}$$

where:

$$\eta_1 = \frac{2Z_c + R_L}{2Z_c R_L C_L} \tag{3.8}$$

$$\eta_2 = \frac{R_L}{2Z_c R_L C_L} \tag{3.9}$$

Finally, substituting Eq. (3.6) and Eq. (3.7) into Eq. (3.1), the equations of 2P TL and 3P TL models, respectively, can be written as:

$$P_C(s) = \frac{e^{\tau s} + \Gamma e^{-\tau s}}{1 + \Gamma} P_F(s) \tag{3.10}$$

$$P_C(s) = \frac{(s + \eta_1)e^{\tau s} + \eta_2 e^{-\tau s}}{s + \eta_1 + \eta_2} P_F(s) \tag{3.11}$$

From Eq. (3.10), it is evident that the 2P TL model is characterized by two parameters. Namely, the pulse transit time, τ, and reflection coefficient, Γ. Similarly, from Eq. (3.11), it is evident that the 3P TL model is characterized by the three parameters τ, η_1, and η_2. Note that these parameters are personalized on an individual basis per subject.

3.2.3 Physiological Relevance of Model Parameters

The TL model parameters hold physiological relevance and may have potential clinical value in monitoring arterial hemodynamics and providing insights into cardiovascular health. For instance, the parameter τ represents the carotid-femoral pulse transit time (or, equivalently, the carotid-femoral pulse wave velocity), which is widely regarded as the gold standard for assessing aortic stiffness [25]. Arterial stiffness is a key biomarker, as it is strongly associated with cardiovascular diseases, making this measurement particularly valuable in clinical settings [25][26].

Additionally, the parameter Γ, known as the reflection coefficient, provides insights into the relative magnitude of the reflected pressure wave, which is also affected by arterial stiffness. This coefficient is important for understanding hemodynamic conditions, as it indicates how much of the pressure wave is reflected toward the heart, which is associated with arterial stiffness. It has been shown that

both the forward and backward waves may hold clinical value in assessing CV health outcomes [27].

Moreover, Γ is related to both the augmentation index (AIx) and pulse pressure amplification (PPA), which are additional biomarkers that are used to assess arterial stiffness [12]. The AIx measures the increase in blood pressure due to the reflected wave, and large AIx values may indicate a greater risk of cardiovascular events (like AAA). A larger Γ may correlate with higher AIx, which provides an alternative way of assessing arterial stiffness and overall cardiovascular health. Similarly, PPA refers to the ratio in pulse pressure between the central and peripheral arteries, which is influenced by wave reflections and transmission dynamics [25]. A larger Γ may indicate greater pulse pressure amplification, as more of the pressure wave is reflected backwards. Since both τ and Γ can be considered similar to existing biomarkers, the TL model parameters provide alternative ways to assess arterial hemodynamic conditions and cardiovascular health, hence bolstering screening and surveillance strategies for AAA.

3.3 Application to AAA

With the understanding that AAA affects BP wave propagation and reflection and that these changes may be reflected in BP waveform morphology, the TL model may be able to differentiate between healthy and aneurysmal aortas by adjusting its parameters appropriately. Considering that AAA largely increases aortic cross-sectional area while moderately increasing aortic stiffness, it is expected that PTT should increase in the presence of AAA. This is consistent with the well-known Moens-Korteweg equation, which is embedded into Eq. (3.2).

The expected direction of change for the reflection coefficient, Γ, is less intuitive to interpret. Initially, it seems reasonable to expect that Γ will decrease in the presence of AAA because the aneurysm will induce a negative wave reflection which may, at least partially, counteract the positive wave reflection that occurs at the distal arteries (which is the primary wave reflection site). However, this holds true only if AAA is considered as a part of the load. In contrast, the TL model captures AAA in its tube, not in its load. Consequently, the TL model reflects AAA as a decrease in characteristic impedance of the tube, which increases the impedance mismatch, leading to an increase in the reflection coefficient [28].

In summary, the TL model parameters may demonstrate physiologically meaningful and explainable differences between healthy individuals and AAA patients. While current methods like ultrasound and CT scans are effective in diagnosing, they are less practical for monitoring. In addition, the one-time screening under the SAAAVE Act has not been effective in preventing rupture [8]. Since the TL model parameters may be different in physiologically expected ways between healthy controls and AAA patients, it may help improve screening and surveillance strategies. If the TL model can effectively be applied to aneurysmal aortas just as well as it can be applied to healthy aortas, then it may serve as a valuable tool in monitoring AAA progression and help to bridge the gap left by today's technologies.

Chapter 4: Tube-Load Model Parameter Estimation

Note: This chapter is based on the author's original work published in [28].

4.1 Experimental Data

The clinical dataset was collected from records of patients with and without AAA at the Taipei Veterans General Hospital between 2010 and 2017 under approval of the Institutional Review Board (IRB) at Taipei Veterans General Hospital. All participants gave written informed consent in accordance with the Declaration of Helsinki. Full details of the study procedure to collect the data are described in our prior work in [29][30].

The patient records contained demographic information, risk factors, hemodynamic data, electrocardiogram (ECG) waveforms, tonometry waveforms from the carotid and femoral arteries, and oscillometric arm-cuff blood pressure measurements. This dataset included over 200 patients with aortic aneurysms (including AAA, thoracic AA, multiple AAs, and aortic dissections) and over 200 patients without aneurysms.

From these >400 records, we selected all records that satisfied our inclusion criteria: (i) AAA patients (i.e., excluding thoracic AA) and (ii) patients without any aortic aneurysm (i.e., control subjects). Our exclusion criteria were patients with: (i) multiple AAs (including aortic dissection), (ii) peripheral arterial disease (PAD), and (iii) artifact-contaminated tonometry waveforms ascertained by visual inspection.

For each patient record, we processed the ECG and tonometry waveforms in several steps. First, we applied a 30 Hz low-pass filter to the ECG signal and a 0.5-10

Hz band-pass filter to the tonometry waveforms. Next, we detected the R waves in the ECG signal using the famous Pan-Tompkins method [31], then used these R waves to segment the carotid and femoral tonometry waveforms into individual beats. We then identified three beats in the tonometry data that were closest in morphology, in terms of beat period and area under the waveform, considering four intervals: (i) R wave to diastolic minimum (pre-ejection period), (ii) diastolic minimum to systolic maximum (systolic upstroke), (iii) systolic maximum to dicrotic notch, and (iv) dicrotic notch to beat end. A visualization of the intervals used to derive the representative carotid and femoral beats is shown below in figure 4-1.

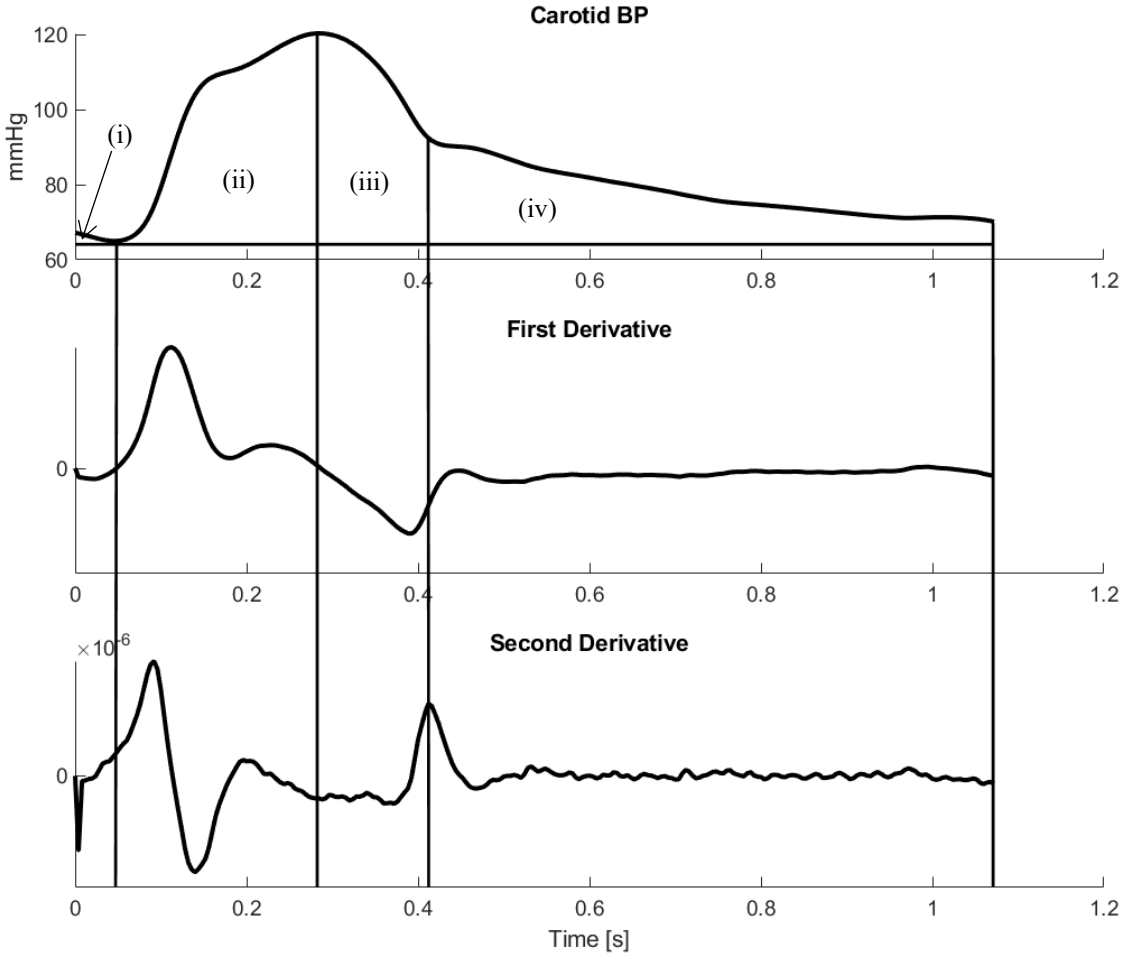

Figure 4-1. Beat period and area features used to derive representative waveforms.

We only considered beats within 12.5% of the median beat period and area values calculated across all beats in the record for each of these four intervals. Finally, we averaged the three selected beats to obtain the representative beat for each patient. The representative beats were then calibrated using the oscillometric arm-cuff's mean and diastolic blood pressure measurements. Patient records that did not contain three similar tonometry beats meeting the above criteria were excluded from further analysis.

A total of 79 AAA patient records and 79 control patient records were derived using the procedure outlined above. We employed a propensity score-based matching technique to systematically select control patients who were similar to the AAA patients in non-waveform characteristics [32]. This matching accounted for potential confounding variables—including age, sex, weight, body surface area (BSA), diabetes status, smoking history, ankle-brachial index (ABI), systolic and diastolic blood pressure, and heart rate—ensuring that the two groups were comparable. We only included male subjects in our study due to differences in the cardiovascular system of male and female subjects. This allows us to better attribute any observed differences in the TL model parameters primarily to the physiological differences between AAA and controls patients instead of baseline demographic and/or health differences. We also selected a subset of 35 AAA patients after receiving EVAR surgery for comparative analysis between pre- and post-EVAR states. The remaining 44 patients were removed from analysis because (i) they did not have representative carotid and/or femoral waveforms or (ii) they were confirmed to have endo-leaks following EVAR via CT scan (i.e., surgery was not successful). Table 4-1

summarizes the demographics, cardiovascular risk factors, and hemodynamic values of the clinical dataset.

It is important to note that some subjects in our study were on medication such as ACE inhibitors and beta-blockers, which are known to affect arterial stiffness. Drug information was incomplete for a significant number of control subjects (38%) in the cohort so these factors could not be accounted for during cohort matching. Additionally, other comorbidities, aside from PAD, were not explicitly accounted for in our matching process. Smoking, which is a significant risk factor for AAA, was accounted for. But conditions like hypertension, hyperlipidemia, and coronary artery disease, which may indicate increased risk of cardiovascular events, were not explicitly controlled for which may have introduced potential confounding effects into our analysis.

Holistically, the control and AAA patient groups were well-matched in all areas that were controlled for except height, where AAA subjects were slightly taller on average. Taller height may lead to larger PTT, although the magnitude of the difference in height was minimal on average (1.2%). Regardless, height may be viewed as a confounding factor in studying the effects of AAA on PTT. As such, we normalized the PTT by height, and other confounding variables, before comparing them between control and AAA subjects to ensure that the effect of height on PTT could be minimized.

Table 4-1: Demographics, CV risk factors, and hemodynamic values of AAA patients, controls subjects ("CON"), and subset of AAA subjects post-EVAR ("EVAR"). *: $p < 0.05$ (unpaired t-test). †: $p < 0.05$ (paired t-test).

	CON (N = 79)	AAA (N = 79 | N = 35)	EVAR (N = 35)
Age [years]	74 ± 8	$77 \pm 10 \mid 76 \pm 11$	78 ± 9
Male, N	79	79 | 35	35
Height [cm]	164 ± 6	$166 \pm 5^{*} \mid 166 \pm 5$	166 ± 5
Weight [kg]	65 ± 10	$65 \pm 10 \mid 65 \pm 8$	64 ± 8
BSA [m^2]	1.7 ± 0.1	$1.7 \pm 0.1 \mid 1.7 \pm 0.1$	1.7 ± 0.1
Diabetes, N	10	6 | 3	3
Smoking, N	26	40 | 17	17
ABI (Right)	1.10 ± 0.09	$1.06 \pm 0.15 \mid 1.04 \pm 0.19$	$0.96 \pm 0.12^{\dagger}$
ABI (Left)	1.07 ± 0.12	$1.05 \pm 0.17 \mid 1.03 \pm 0.20$	$0.97 \pm 0.13^{\dagger}$
SBP [mmHg]	130 ± 17	$132 \pm 17 \mid 132 \pm 17$	126 ± 18
DBP [mmHg]	74 ± 9	$75 \pm 10 \mid 74 \pm 10$	$70 \pm 10^{\dagger}$
HR [bpm]	65 ± 10	$64 \pm 12 \mid 63 \pm 9$	$70 \pm 13^{\dagger}$
AAA Diameter [cm]	-	5.5 ± 1.3	-

4.2 Model Fitting and Parameter Estimation

For each patient within the clinical dataset, we fitted two variants of the TL model (namely, the 2P and 3P TL models) to the carotid and femoral artery tonometry waveforms on an individual basis. We first transformed the 2P and 3P TL models into their discrete-time difference equations using the Euler approximation: $s \cong (q-1)F_s$, where q is the forward shift operator and F_s is the sampling frequency

of the tonometry waveforms (250 Hz). The discrete-time domain equation of the 2P model is given by:

$$P_C(k) = \frac{1}{1+\Gamma} P_F(k+n) + \frac{\Gamma}{1+\Gamma} P_F(k-n) \tag{4.1}$$

and the discrete-time domain equation of the 3P model is given by:

$$P_C(k+1) = \left(1 - \frac{\eta_1 + \eta_2}{F_s}\right) P_C(k) + P_F(k+n+1) + \left(\frac{\eta_1}{F_s} - 1\right) P_F(k+n) + \frac{\eta_2}{F_s} P_F(k-n) \tag{4.2}$$

where PTT τ was approximated as the equivalent discrete-time delay $n = \tau F_s$. Next, we inputted the time series sequence of the femoral artery tonometry waveforms into the TL model in the discrete-time domain to compute the corresponding time series sequence of the carotid artery tonometry waveform. We then optimized the TL model parameters to minimize the root mean squared error (RMSE) between the measured carotid waveform and the carotid waveform estimated by the TL model.

To maximize accuracy and minimize uncertainty in estimating the parameters, we employed an exhaustive search method. In the case of the 2P TL model, we exhaustively searched over physiologically realistic yet still conservative ranges of τ and (10-160 ms) and Γ (0-1). In the case of the 3P TL model, we performed exhaustive search on τ—which is more sensitive and identifiable than Γ—and invoked a numerical optimization procedure using "FMINCON" from MATLAB Optimization Toolbox to infer optimal values of η_1 and η_2 for each value of τ considered. The optimal values of τ, η_1, and η_2 were determined as those associated with the smallest RMSE. Finally, we computed the optimal estimated carotid waveform replicated by the TL model by inputting the femoral artery waveform into

the TL model in the discrete-time domain personalized with the optimal parameter values.

It is important to note that while the parameter τ can be bracketed using physiology, the parameters related to the reflection coefficient require proper constraints. In particular, Γ of the 2P TL model is bounded between 0 and 1 which signifies minimum and maximum pulse pressure amplification. In the case of the 3P TL model, η_1 and η_2 are related to the arterial compliance, resistance, and tube characteristic impedance, which are physical quantities. So, for these parameters, a lower bound of 0 is set. Additionally, η_1 and η_2 should not become too large to ensure system stability. Specifically, we ensure that the discrete system poles lie within the unit circle by constraining η_1 and η_2 in the optimization. The constraints on Γ, along with η_1 and η_2 to conduct the optimization routine are:

$$0 \leq \Gamma \leq 1 \tag{4.3}$$

$$\eta_1 \geq 0, \eta_2 \geq 0 \tag{4.4}$$

$$-1 \leq \frac{\eta_1 + \eta_2}{F_s} \leq 1 \tag{4.5}$$

As established in Chapter 3, the TL model parameters, τ and Γ, depend on the aortic radius r_T and elastic modulus E, which are two critical factors governing the behavior of AAA. Thus, the TL model can account for these factors and their influence on BP wave propagation and reflection in the aorta. Additionally, the parameter Γ depends on blood pressure and age, whereas τ depends on blood pressure, age, and height. Moreover, both parameters are influenced by load impedance characterized by R_L and C_L. As such, τ and Γ represent the collective

influence of all these factors on blood pressure wave propagation and reflection in the aorta. These factors may exhibit significant inter- and intra-individual variability in their effect on τ and Γ, which can be accounted for by estimating the TL model parameters each time new measurements are obtained from an individual patient.

Chapter 5: Evaluation of Tube-Load Models as Digital Twins

Note: This chapter is based on the author's original work in [28].

5.1 Results

For all comparisons, we used the unpaired t-test to determine the statistical significance of observed differences in control and AAA subjects, whereas in the case of pre- and post-EVAR AAA subjects, we used the paired t-test to determine statistical significance.

5.1.1 Parameter Normalization

The goodness of fit between the measured and estimated carotid waveforms, as well as the differences in TL model parameters were compared between control and AAA subjects (N = 79) and AAA subjects before and after EVAR (N = 35). The goodness of fit was evaluated using the RMSE and correlation coefficient (i.e., r value) between the measured and estimated carotid waveforms for each subject.

The TL model parameters were compared after normalizing for cofactors to minimize their influence on the differences observed among control, AAA and post-EVAR AAA subjects. Qualitatively, increased blood pressure and age decrease arterial compliance. This reduction in compliance leads to a decrease in PTT by increasing PWV. It also decreases the reflection coefficient, as well as $\eta_1 \; and \; \eta_2$, by increasing characteristic impedance. Additionally, PTT may be proportional to the distance between tonometry measurement sites at the carotid and femoral arteries. Although these variables were accounted for through a systematic approach to cohort matching, residual effects may still be present. So, PTT was normalized by

multiplying by blood pressure and age and dividing by height. Likewise, the reflection coefficient Γ, along with η_1 and η_2, was normalized by multiplying by blood pressure and age.

The normalization method is quantitatively reasonable for several reasons. According to the well-known Bramwell-Hill equation, PTT may have a curvilinear inverse relationship with blood pressure and an approximately linear inverse relationship in the high blood pressure regime [33], which gives the relation $\tau \sim BP^{-1}$. Additionally, literature indicates that PWV (which is inversely proportional to PTT) is approximately proportional to age, suggesting that $\tau \sim age^{-1}$ [25]. And as Eq. (3.11) indicates, PTT is directly proportional to the aortic inlet-outlet distance, so $\tau \sim d$. Similarly, Eq. (3.3) leads to the following relationship:

$$1 - \Gamma = \frac{2Z_C}{Z_L + Z_C} = \left(\frac{1}{2} + \frac{Z_L}{2Z_C}\right)^{-1} \sim Z_C \tag{5.1}$$

Since $Z_C = \sqrt{\frac{l_l}{c_l}} = l_l\sqrt{\frac{1}{l_l c_l}}$ and combined with Eq. (3.2) gives:

$$Z_C = l_l \frac{d}{\tau} \tag{5.2}$$

which makes clear that Z_C is inversely proportional to PTT, so $1 - \Gamma \sim Z_C \sim d/\tau$. Now, using the dependence of τ on blood pressure and age, it can be established that $1 - \Gamma \sim BP$ and $1 - \Gamma \sim age$. Thus, giving the relationship of RC with BP and age as $\Gamma \sim BP^{-1}$ and $\Gamma \sim age^{-1}$, respectively. Therefore, multiplying by blood pressure and age for RC, and multiplying by blood pressure and age and dividing by height for PTT may be a reasonable approach to account for their effects on PTT and RC.

5.1.2 Goodness of Fit

Table 5-1 summarizes the goodness of fit between the measured carotid waveform and the estimated carotid waveform from the TL model personalized with the optimal parameters. Figure 5-1 shows representative examples of the measured and estimated carotid waveforms from both the 2P and 3P TL models for 3 control, 3 AAA, and 3 post-EVAR subjects across a wide range of aneurysm diameters.

*Table 5-1: Goodness of fit of the 2P and 3P TL models for CON, AAA, and EVAR recordings. *: $p < 0.05$ (unpaired t-test).*

		CON (N = 79)	AAA (N = 79 | N = 35)	EVAR (N = 35)
2P TL	RMSE [mmHg]	3.0 ± 1.8	$2.6 \pm 1.1 \mid 2.3 \pm 0.9$	2.2 ± 1.2
	r	0.95 ± 0.05	$0.99 \pm 0.01 \mid 0.99 \pm 0.01$	0.99 ± 0.01
3P TL	RMSE [mmHg]	$2.7 \pm 2.1^{*}$	$2.1 \pm 1.1 \mid 1.9 \pm 0.8$	1.7 ± 1.2
	r	$0.95 \pm 0.05^{*}$	$0.99 \pm 0.01 \mid 0.99 \pm 0.01$	0.99 ± 0.00

Overall, both the 2P and 3P TL models fit equally well to control, AAA, and post-EVAR subjects. Interestingly, however, the TL model showed a tendency to fit AAA subjects better than control subjects. On average, the RMSE between the measured and estimated carotid waveforms was small, deviating less than 2.2% relative to the mean blood pressure level. Additionally, the correlation coefficient between the measured and estimated carotid waveforms was remarkably high at over 0.95. Among the 79 control subjects, 79 AAA subjects, and the subset of 35 pre- and post-EVAR subjects, no differences were statistically significant—except between control and AAA subjects for the 3P TL model. In this case, the differences in RMSE

and correlation coefficient were marginally significant, with p-values of 0.04 and 0.02, respectively.

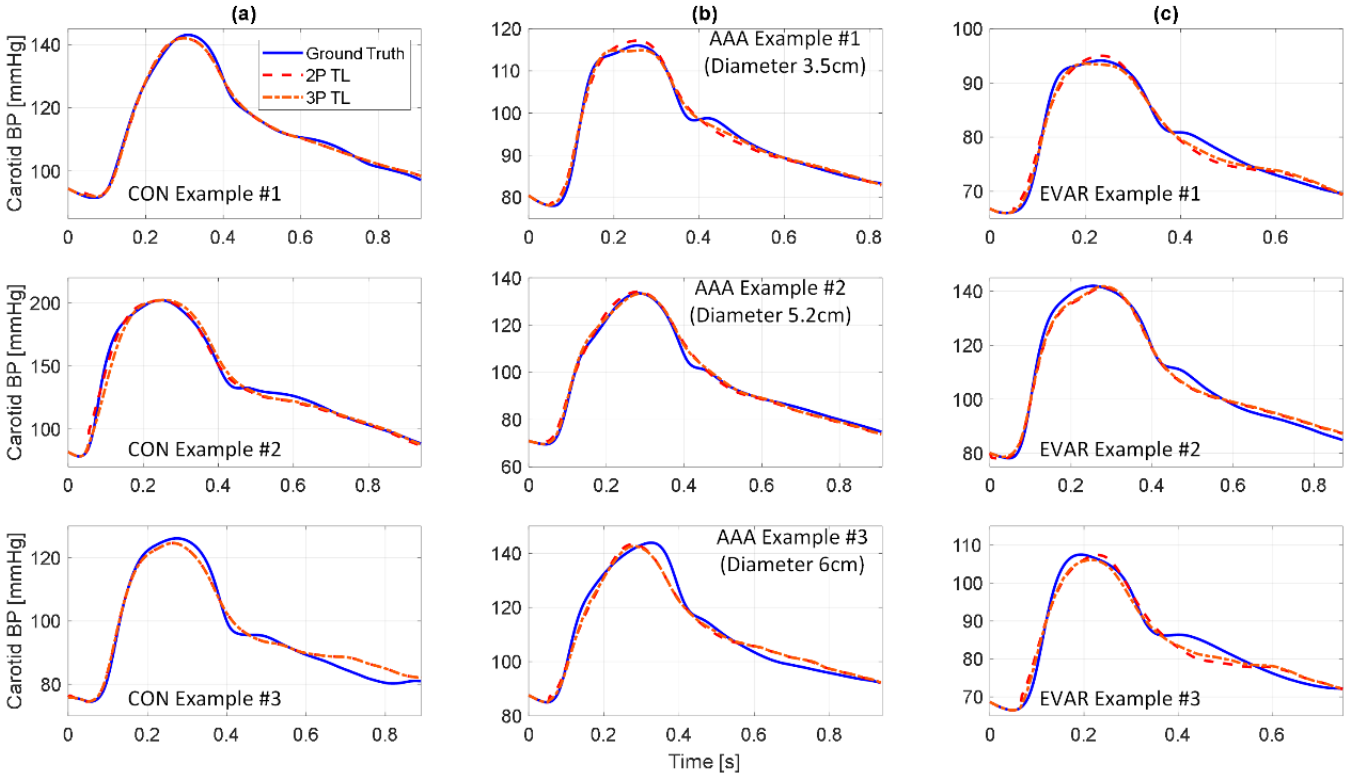

Figure 5-1. Representative examples of measured carotid waveform vs. estimated waveform replicated by the two TL model variants when femoral artery waveform was input for (a) 3 controls, (b) 3 AAA and (c) 3 post-EVAR subjects.

5.1.3 Tube-Load Model Parameters

After assessing the goodness of fit of the estimated waveforms, we next analyzed the estimated parameters across the control, AAA and post-EVAR subjects to understand how aneurysmal and post-surgical changes influence physiological properties of the aorta. In general, the normalized PTT and reflection coefficients were larger in AAA subjects than in control subjects. As previously explained in chapter 3, this is the expected direction of change physiologically speaking. Table 5-2 summarizes the mean and standard deviation of the TL model parameters across these

groups, while table 5-3 summarizes the normalized parameters. Figure 5-2 compares the normalized PTT of control vs. AAA and pre- vs. post-EVAR subjects for both the 2P and 3P TL models. Figure 5-3 compares the normalized reflection coefficient, as well as normalized η_1 and η_2 of control vs. AAA and pre- vs. post-EVAR subjects for both the 2P and 3P TL models. It is worth noting that the reflection coefficient for the 3P TL model is a function of frequency, while the reflection coefficient for the 2P TL is a constant. So, for the 3P TL model only, the magnitude of the reflection coefficient at the heart rate frequency was used in analyzing the reflection coefficient values.

Figure 5-4 compares the subject-specific pulse transit time estimated via the 2P and 3P TL models and the subject-specific pulse transit time measured directly from the carotid and femoral artery tonometry waveforms. When not normalized, the 2P TL PTT showed $r = 0.60$ for AAA subjects and $r = 0.70$ for control subjects. The 3P TL PTT showed $r = 0.80$ for AAA subjects and $r = 0.86$ for control subjects. Likewise, figure 5-5 shows the subject-specific normalized pulse transit time estimated via the 2P and 3P TL models and the equivalent normalized pulse transit time measured directly from the carotid and femoral artery tonometry waveforms. When normalized, the 2P TL PTT showed $r = 0.68$ for AAA subjects and $r = 0.65$ for control subjects. The 3P TL PTT showed $r = 0.84$ for both the AAA and control subjects.

The TL model PTT shows a high degree of correlation with the measured PTT indicating that the TL model may be an effective way to estimate PTT. Figure 5-6 shows the correlation between normalized PTT and reflection coefficient of the 2P

and 3P TL models to aneurysm size. Normalized PTT exhibited $r = 0.40$ and $r = 0.45$ for the 2P and 3P TL models, respectively. In contrast, the normalized reflection coefficient exhibited $r = 0.05$ and $r = 0.07$ for the 2P and 3P TL models, respectively. The stronger correlation between PTT and AAA size may be partly attributed to the stronger practical identifiability of PTT compared to RC (see discussion).

Table 5-2

: TL model parameters pertaining to control, AAA, and post-EVAR subjects for 2P and 3P TL models.

		CON (N = 79)	AAA (N = 79 | N = 35)	EVAR (N = 35)
2P TL	τ [ms]	52.6 ± 13.8	52.9 ± 12.7 | 52.9 ± 13.5	$47.2 \pm 15.6^{\dagger}$
	Γ	0.22 ± 0.21	0.33 ± 0.23 | 0.32 ± 0.23	$0.22 \pm 0.19^{\dagger}$
3P TL	τ [ms]	48.9 ± 11.3	49.5 ± 11 | 49.4 ± 10.3	$43.9 \pm 13^{\dagger}$
	Γ	0.24 ± 0.22	0.33 ± 0.23 | 0.32 ± 0.24	0.23 ± 0.20
	η_1	57.6 ± 100.4	102 ± 139 | 106 ± 140	$21.2 \pm 27.7^{\dagger}$
	η_2	9.21 ± 15.4	19.8 ± 27.1 | 20.1 ± 27.4	$4.80 \pm 5.11^{\dagger}$

*: Significantly different from controls ($p < 0.05$ unpaired t-test). †: Significantly different from pre-EVAR ($p < 0.05$ paired t-test).

Table 5-3: Normalized TL model parameters pertaining to control, AAA, and post-EVAR subjects for 2P and 3P TL models.

		CON (N = 79)	AAA (N = 79 | N = 35)	EVAR (N = 35)
2P TL	$\tau \left[\frac{s \cdot mmHg \cdot years}{cm}\right]$	2.27 ± 0.60	2.37 ± 0.58 | 2.34 ± 0.60	$1.98 \pm 0.64^{\dagger}$
	Γ [mmHg·years]	1572 ± 1564	$2551 \pm 2073^{*}$ | 2562 ± 2115	$1552 \pm 1494^{\dagger}$
3P TL	$\tau \left[\frac{s \cdot mmHg \cdot years}{cm}\right]$	2.11 ± 0.48	2.22 ± 0.57 | 2.19 ± 0.53	$1.85 \pm 0.52^{\dagger}$
	Γ [mmHg·years]	1677 ± 1629	$2562 \pm 2052^{*}$ | 2524 ± 2222	1621 ± 1635
	η_1 [mmHg·years]	$4351E2 \pm 7608E2$	$7717E2 \pm 1060E2^{*}$ | $7598E2 \pm 9569E2$	$1406E2 \pm 1784E2^{\dagger}$
	η_2 [mmHg · years]	$6571E1 \pm 1079E2$	$1552E2 \pm 2142E2^{*}$ | $1557E2 \pm 2235E2$	$32211 \pm 32641^{\dagger}$

*: Significantly different from controls ($p < 0.05$ unpaired t-test). †: Significantly different from pre-EVAR ($p < 0.05$ paired t-test).

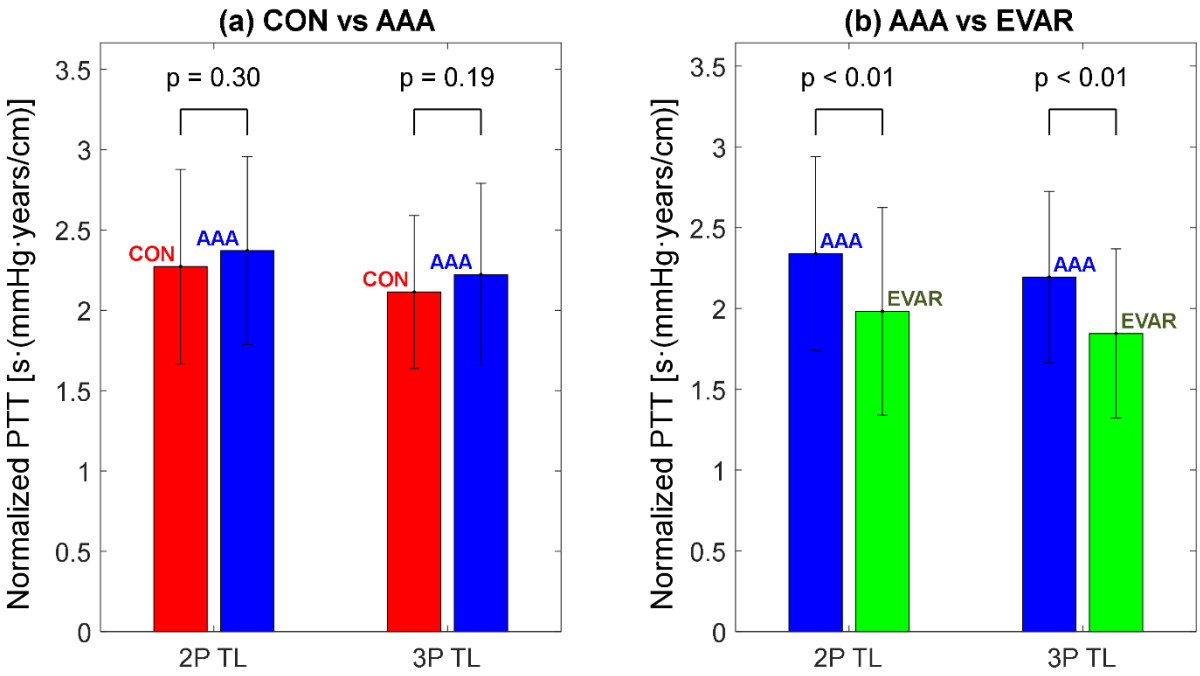

Figure 5-2. Normalized PTT in control vs. AAA subjects and pre- vs. post-EVAR subjects for the 2P and 3P TL models. (a) depicts control vs. AAA and (b) depicts pre- vs. post-EVAR comparison.

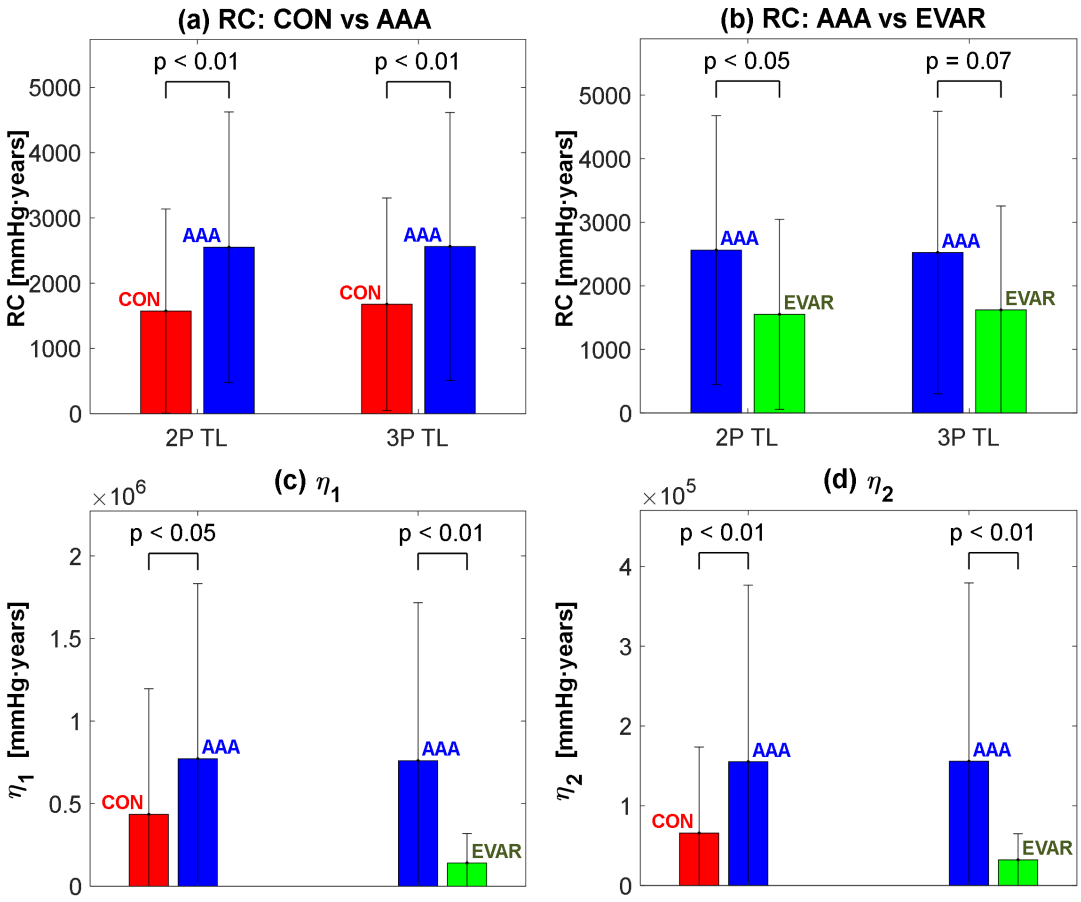

Figure 5-3. Normalized RC, as well as η_1 and η_2 in control, AAA, and post-EVAR subjects for the 2P and 3P TL models. (a) depicts normalized RC for control vs. AAA, and (b) depicts normalized RC for pre- vs. post-EVAR. (c) depicts normalized η_1 for control vs. AAA and pre-vs post-EVAR, and (d) depicts normalized η_2 for control vs. AAA and pre- vs. post-EVAR.

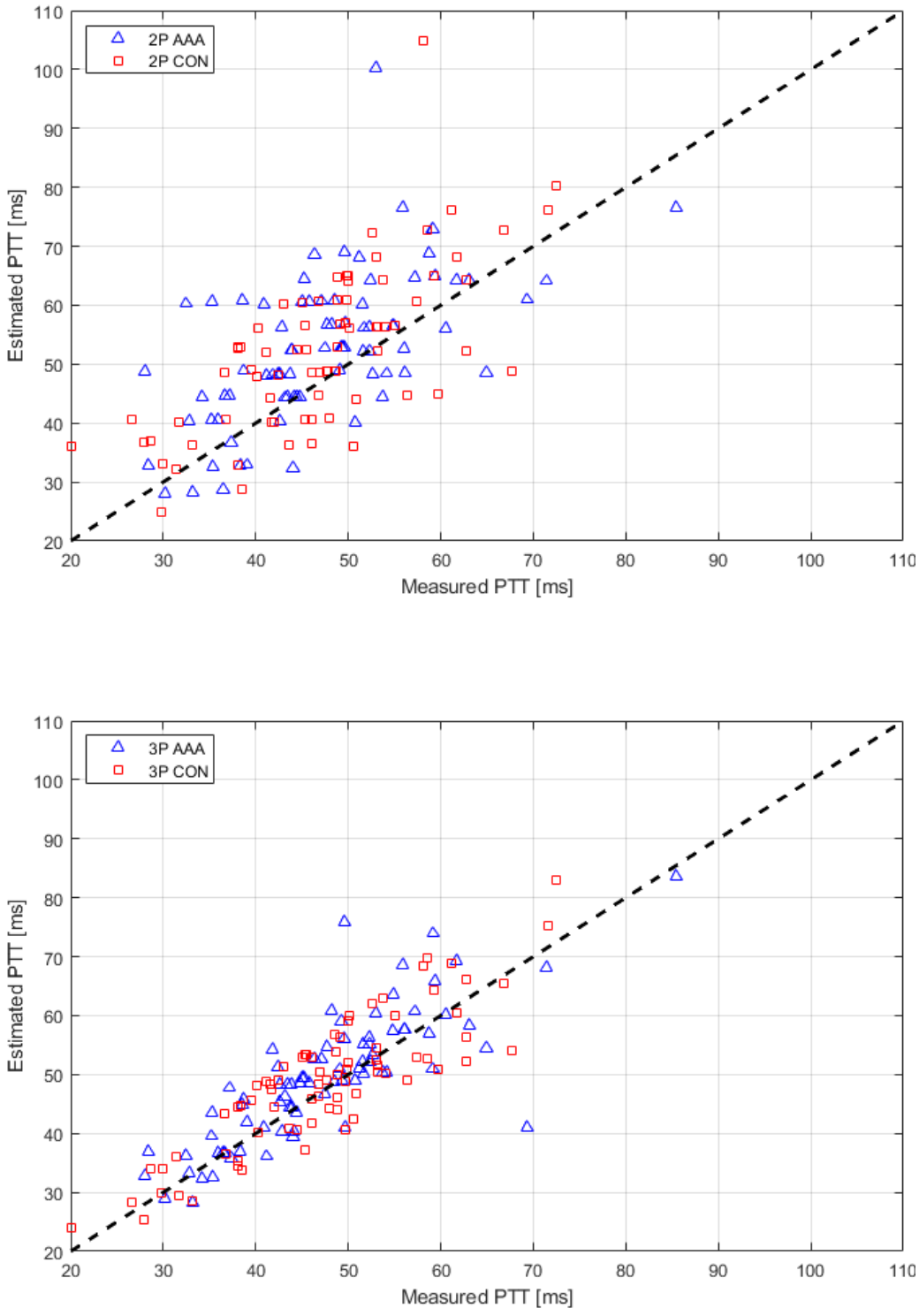

Figure 5-4. Comparison of estimated PTT from the 2P and 3P TL models and the measured PTT directly from the carotid and femoral artery tonometry waveforms. Black lines drawn are the identity lines.

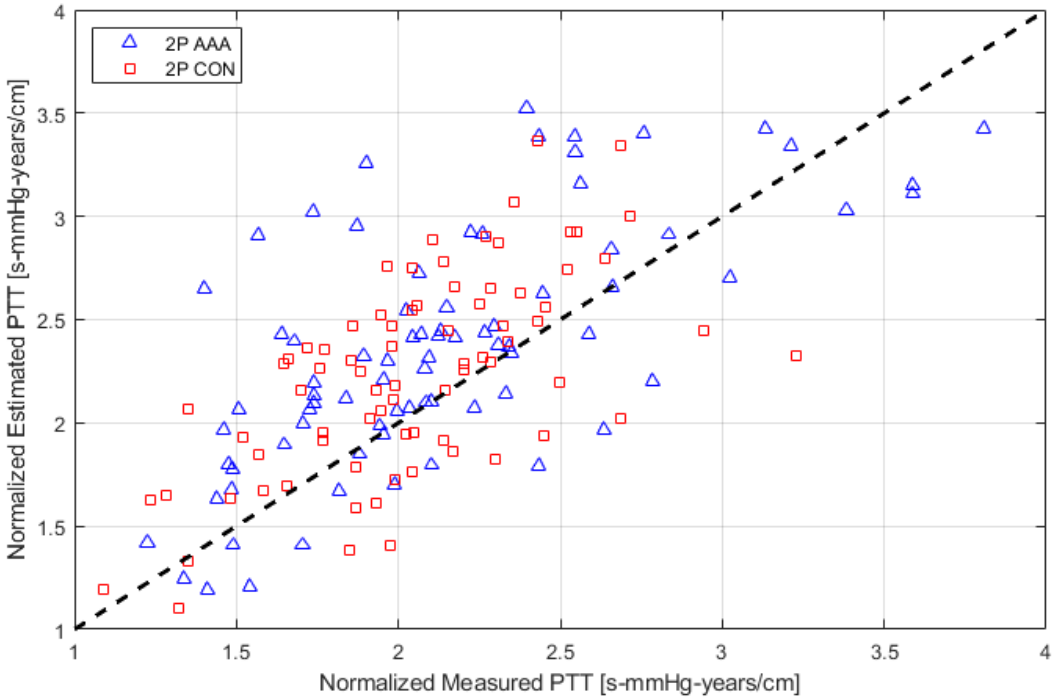

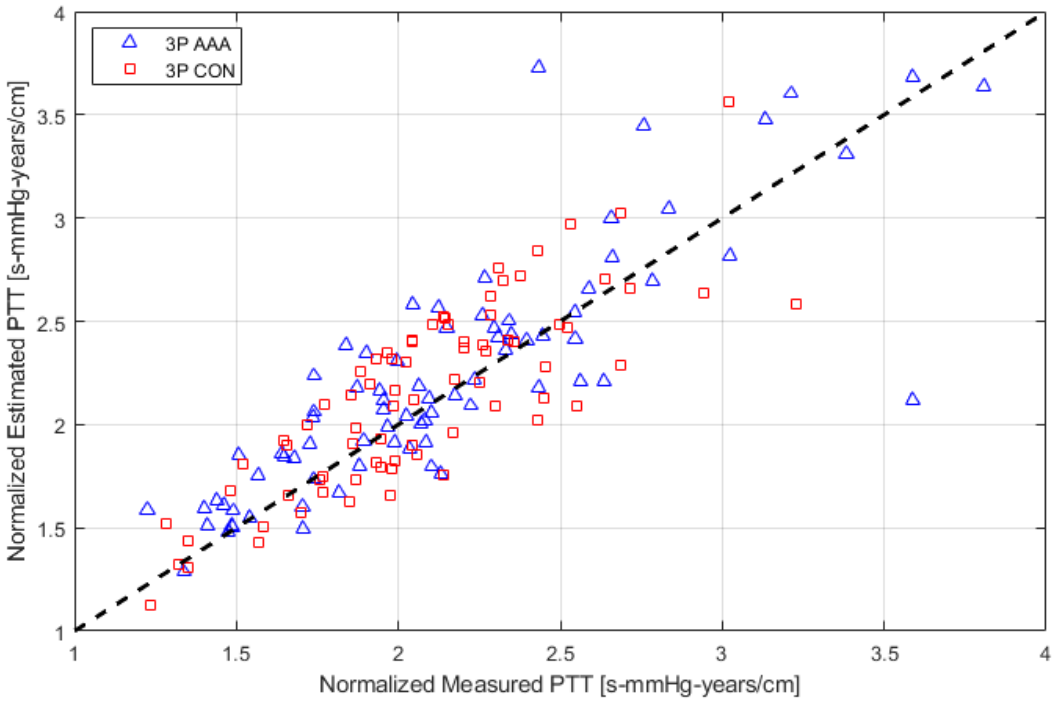

Figure 5-5. Comparison of normalized estimated PTT from the 2P and 3P TL models and the normalized measured PTT directly from the carotid and femoral artery tonometry waveforms. Black lines drawn are the identity lines.

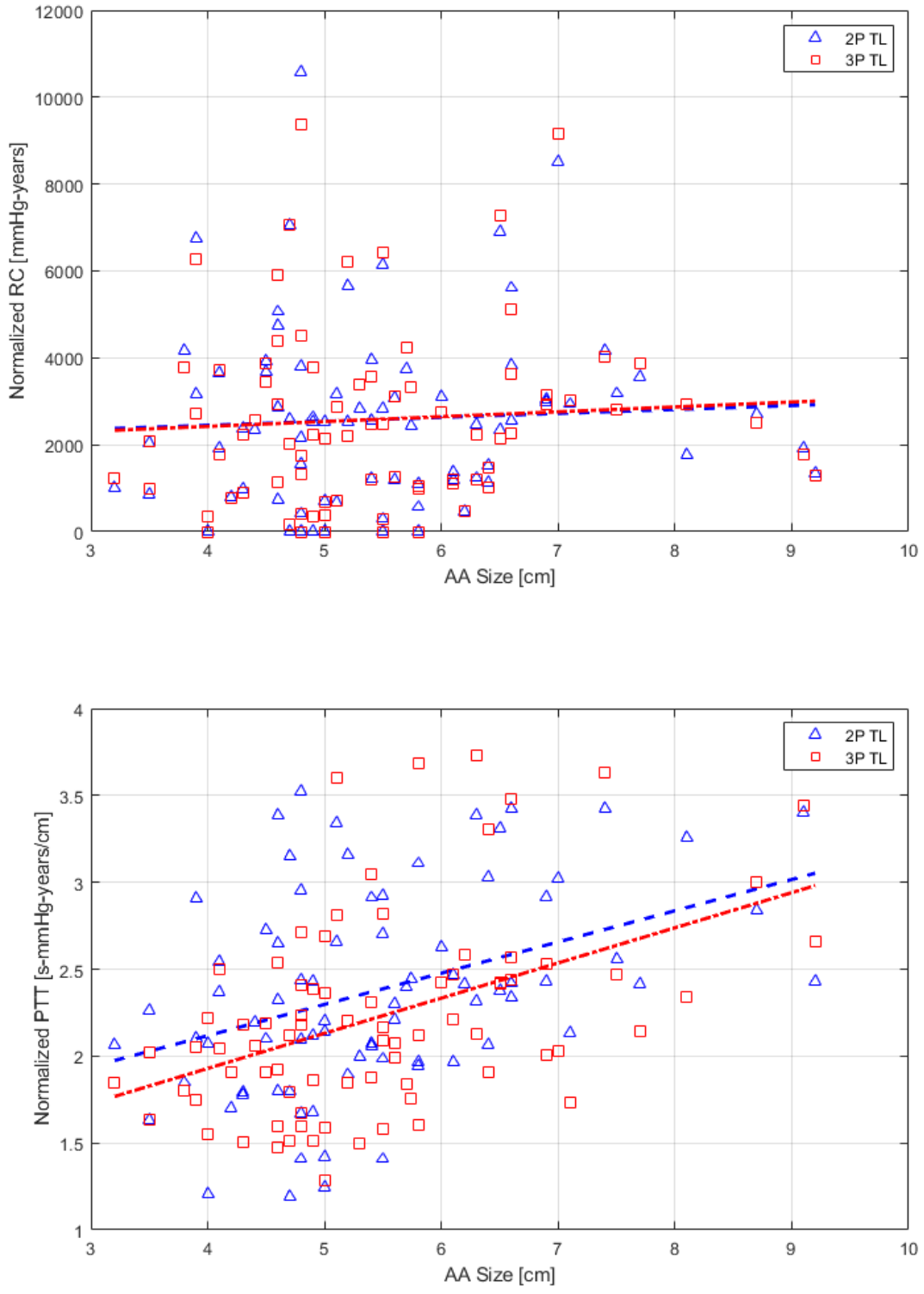

Figure 5-6. Correlation of normalized PTT and normalized reflection coefficient of the 2P and 3P TL models with AAA size. Blue and red lines drawn are the least squares regression line for the 2P and 3P TL models, respectively.

5.1.4 Feasibility of AAA Diagnosis

We conducted a logistic regression analysis using a leave-one-subject-out approach to evaluate the efficacy of the TL model parameters in distinguishing between control and AAA subjects, as well as AAA subjects pre- and post-EVAR. Figure 5-7 shows the results of the logistic regression analysis. The results suggest that the TL model parameters, once normalized, show modest potential in diagnosing AAA and assessing the success of EVAR procedure. Using all normalized parameters of the 3P TL model (i.e., τ, Γ, η_1 and η_2), we achieved receiver operating characteristic (ROC) area under the curve (AUC) values of 0.67 for classifying control versus AAA subjects, and 0.78 for classifying AAA subjects pre- versus post-EVAR. At a 75% specificity level, the TL model parameters had a sensitivity of 50% in classifying control versus AAA subjects, and 68% in classifying AAA subjects pre- versus post-EVAR. This is comparable to the 39%-68% sensitivity of aortic palpation at the same specificity level, which requires trained experts [2].

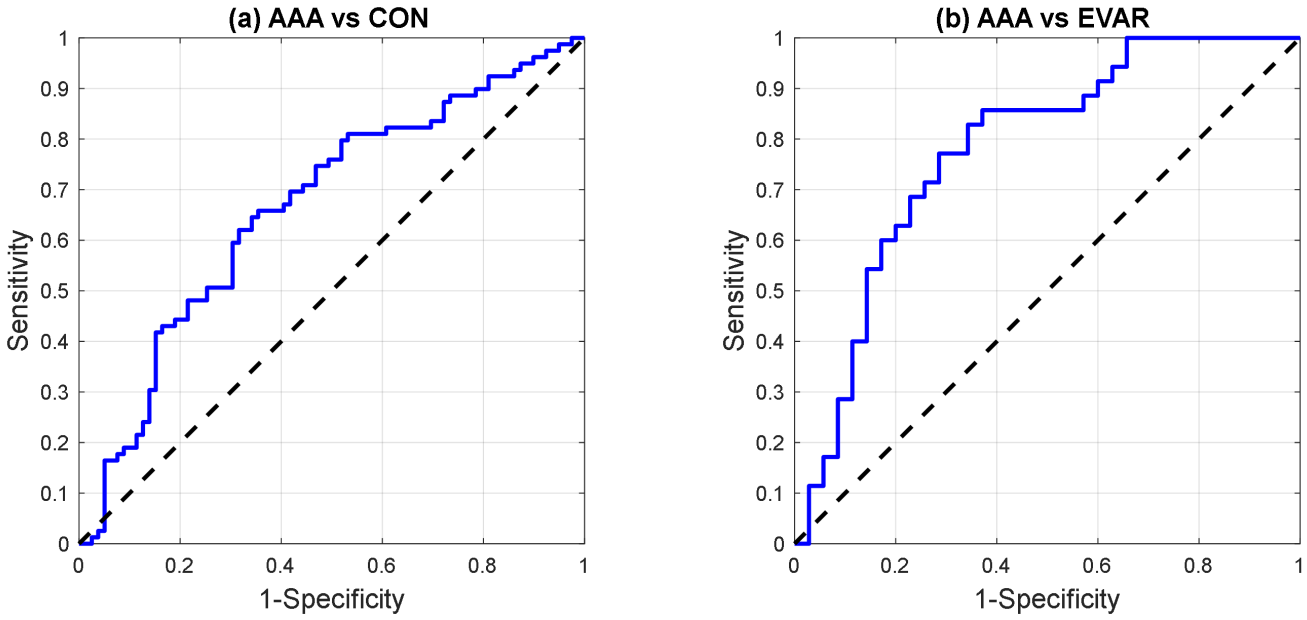

Figure 5-7. Receiver operating characteristics (ROC) pertaining to classifying (a) control versus AAA subjects and (b) AAA subjects before and after EVAR.

5.2 Discussion

In general, both the 2P and 3P TL models were capable of fitting to AAA subjects before and after EVAR surgery, as well as their matched control subjects equally well. However, the 2P model exhibited significantly superior goodness of fit regarding RMSE and correlation coefficient than control subjects (table 5-1 and figure 2). It has been established that the TL model is a valid and effective representation of disease-free arteries including the aorta [22][34]-[36]. Since aneurysmal aortas violate the assumption that aortic cross-sectional area is monotonically decreasing (or constant), we suspected that a more complex, multi-segmented TL model would be necessary to fit the carotid and femoral artery tonometry waveforms.

However, it turned out that a single-segment uniform lossless TL model was sufficient. The results suggest that a single-segment uniform lossless TL model not only has the ability to fit to aneurysmal aorta, but also the ability to elucidate AAA-induced changes to blood pressure wave propagation and reflection via its parameters. The results also suggest that more sophisticated TL models may not significantly improve the goodness of fit while simultaneously introducing unnecessary challenges associated with accurately estimating the additional parameters.

An important point of discussion is that, counterintuitively, the goodness of fit of control subjects was worse than that of AAA subjects, as shown in table 5-1 and figure 5-1. Further investigation revealed that there were more control subjects with reflection coefficient values equal to 0 compared to AAA subjects. In the case of the 2P TL model, 22 control subjects had a reflection coefficient value of 0, compared to

only 9 AAA subjects. Similarly, in the 3P TL model, 17 control subjects had a reflection coefficient value of 0, compared to only 5 AAA subjects. Closer examination of the dataset revealed that most of these subjects were associated with pulse pressure attenuation (i.e., femoral artery pulse pressure was smaller than carotid artery pulse pressure). For the 2P TL model, 83% of control subjects and 89% of AAA subjects with reflection coefficient of 0 showed pulse pressure attenuation. In the 3P TL model, this proportion rose to 94% for controls and 100% for AAA subjects.

These findings are physiologically unexpected, since pulse pressure typically amplifies as blood pressure propagates. We speculate that the pulse pressure attenuation observed in our dataset could be due to several factors, including (i) measurement error in carotid artery tonometry, (ii) measurement error in femoral artery tonometry and (iii) calibration error in the tonometry waveforms. However, the exact and dominant cause leading to pulse pressure attenuation in the affected subset of subjects remains unknown.

In the context of blood pressure wave propagation and reflection dictated by the TL model, only pulse pressure amplification can be replicated, not attenuation. As such, the TL model may have been forced to set the reflection coefficient to 0 in these subjects. Consequently, this may deteriorate the goodness of fit of the TL model. Given that there were more control subjects with reflection coefficient of 0 than AAA subjects, it is plausible that the RMSE in control subjects may be worse than AAA subjects.

As established in chapter 3, the TL model parameters may exhibit physiologically explainable differences between control and AAA subjects. The results support this claim. First, after normalizing for mean blood pressure, age, and height, PTT was smaller in control subjects than in AAA subjects. Additionally, PTT was smaller in post-EVAR subjects than in pre-EVAR subjects, which further aligns with expectations since the hemodynamic state typically returns to normal post-EVAR, resembling that of control subjects. These findings are consistent with prior work and align with physiological expectations based on the well-known Moens-Korteweg equation [30][37]. Second, after normalizing for mean blood pressure and age, the reflection coefficient (along with η_1 and η_2), was found to be smaller in control subjects than in AAA subjects.

Initially, it may seem counterintuitive that reflection coefficient increases with AAA. The aortic expansion at the aneurysm site results in negative wave reflection which could partially counteract the positive wave reflection occurring at the primary wave reflection site, the distal arteries [38]. Thus, one might expect the reflection coefficient to be larger in control subjects than in AAA subjects, as well as larger in post-EVAR subjects than in pre-EVAR subjects. However, this expectation holds only when the AAA is considered as a part of the load. In contrast, the TL model treats the AAA as a part of its tube by the decrease in characteristic impedance Z_C. This increases the impedance mismatch between the tube and the load thereby increasing the reflection coefficient.

In summary, both the differences in PTT and reflection coefficient observed between control and AAA subjects, as well as pre- and post-EVAR subjects are

physiologically explainable given that the TL model treats the AAA as a part of its tube. The aneurysm-induced aortic expansion largely increases the arterial compliance c_l while moderately decreasing arterial inertance l_l. Since the increase in c_l dominates the decrease in l_l, PTT increases in the presence of AAA, as predicted by Eq. (3.2). Additionally, the combined increase in c_l and decrease in l_l due to AAA decreases the characteristic impedance Z_C without affecting the load impedance characteristics R_L and C_L, leading to an increase in the reflection coefficient (along with η_1 and η_2), as predicted by Eq. (3.3) and (3.7). The results support the notion that the TL model can capture AAA-induced changes to blood pressure wave propagation and reflection through its parameters, namely τ and Γ from the analysis of non-invasive carotid and femoral artery tonometry waveforms.

The results shown in figures 5-2 and 5-3 are remarkable (except for the lack of statistical significance in PTT between control and AAA subjects) since they remain consistent with prior research and physiological expectations. In particular, the statistical significance of PTT and reflection coefficient differences between pre- and post-EVAR subjects is notable, especially given the relatively small sample size of just 35 subjects. In addition to their differences being consistent with physiology, the pre- and post-EVAR subjects were the same person measured at two different points. This means that each pre- and post-EVAR subject serves as their own control, minimizing the interindividual variability. As such, the pre- and post-EVAR analysis results may not be seriously subject to any bias.

It is worth noting that PTT between control and AAA subjects was not significantly different (in neither the 2P nor 3P TL models) but was significantly

different between pre- and post-EVAR subjects. It is possible that the graft material used to repair the aneurysm in the EVAR procedure affected the PTT following EVAR by stiffening the aorta. Prior work shows that the stent may have an influence in increasing the pulse wave velocity, although the effect may not be substantial [30][39][40]. In any case, the relative decrease in PTT in the post-EVAR subjects compared to pre-EVAR subjects may reflect the combined effect of aneurysm repair and graft material. This may explain the larger and statistically significant differences observed in PTT between pre- and post-EVAR subjects compared to the control and AAA subjects.

Another aspect of the results worth addressing is the statistically significant difference in reflection coefficient (along with η_1 and η_2), contrasted with the statistically insignificant difference in PTT between the control and AAA subjects. Eq. (3.2) indicates that $\tau^2 \sim r_T$, meaning that PTT is proportional to the square root of the aortic radius. Similarly, Eq. (3.3) suggests that $Z_C^2 \sim r_T^{-5}$, meaning that characteristic impedance is inversely proportional to $\sqrt{r_T^5}$. Hence, according to Eq. (3.6) and (3.7), reflection coefficient is roughly proportional to $\sqrt{r_T^5}$. Additionally, since $\eta_1 = \frac{1}{R_L C_L} + \frac{1}{2Z_C C_L} \sim \frac{1}{Z_C}$ and $\eta_2 = \frac{1}{2Z_C C_L} \sim \frac{1}{Z_C}$ which lead to the conclusion that η_1 and η_2 are also proportional to $\sqrt{r_T^5}$. As such, both the reflection coefficient and the parameters η_1 and η_2 may exhibit larger changes to AAA-induced increase in arterial radius compared to PTT. This may mean that the reflection coefficient (along with η_1 and η_2) may be more sensitive to AAA compared to PTT.

A related issue may involve the practical identifiability of the parameters within the TL model. It is known that PTT is more readily identifiable than the reflection coefficient [41][42]. Furthermore, according to the theory of blood pressure wave propagation and reflection, pulse pressure amplification between the carotid and femoral arteries tends to increase either the PTT and/or the reflection coefficient. Consequently, the TL model parameters τ and Γ may vary in opposite directions to best replicate the observed pulse pressure amplification. With these considerations, it is possible that a subset of subjects may be affected by errors related to the lack of practical identifiability of the parameters. Specifically, the PTT could have been overestimated (or underestimated) while reflection coefficient was underestimated (or overestimated). Such shifts in the parameter values may have contributed to weakening the statistical significance in the differences observed in PTT between control and AAA subjects.

A crucial step in analyzing the TL model parameters is parameter normalization. PTT is known to be influenced by factors such as blood pressure, age, and height, making it essential to remove these effects to accurately interpret the impact of AAA on PTT [33]. Interestingly, most prior studies investigating the effect of AAA on PTT (or equivalently PWV) have found a decrease in PTT in the presence of AAA. This effect may stem from the confounding influences of blood pressure and age that were not adequately accounted for prior to analysis [40][43]-[46].

In this work, control and AAA subjects were matched rigorously and systematically, as detailed in chapter 4 and table 4-1, to account for interindividual variability as best as possible. Although factors like medication use and comorbidities

were not considered, we observed that the differences in PTT without normalization were minimal on average between control and AAA subjects, as shown in table 5-2. Only after normalization did the differences in PTT between control and AAA subjects were clearly visible. Additionally, after normalizing, we observed that the p-value of the reflection coefficient in both the 2P and 3P TL models decreased by over threefold, while the p-value of the parameter η_2 decreased by over twofold. This highlights the importance of normalizing the parameters to clearly elucidate the effect of AAA on the TL model parameters in an explainable way.

Another potential use for the TL model parameters is in predicting the severity of aneurysm diameters which may help in determining if surgical intervention is necessary. However, in this study, we only have information on the maximum aneurysm diameter and not on diameter changes over time. Additionally, post-operative diameter measurements are unavailable, limiting our ability to assess the TL model's capability in predicting the progression or severity of AAA. Despite the limitations in data, as shown in figure 5-6, the TL model estimated PTT demonstrated a moderate correlation (r = 0.4 for 2P TL and r = 0.45 for 3P TL) with maximum aneurysm size. This finding suggests that the parameter τ may capture physiological characteristics that are relevant to aneurysm severity. While these results are promising, the lack of temporal diameter data limits our ability to assess how well the TL model could predict changes in aneurysm size or severity over time. Incorporating longitudinal measurements in future studies could further clarify the relationship between the TL model parameters and aneurysm progression.

Regarding the potential to detect AAA, the 3P TL model parameters showed superior performance to the 2P TL model parameters in classifying AAA versus control subjects, as shown in figure 5-7. This may be due to the larger number of features that are usable by the classification model which may provide more information leading to better classification performance. Despite the superior classification performance with the 3P TL model, the 2P TL model may still offer some advantages in certain contexts. For one, the 2P TL model is simpler with only 2 parameters, making it possible to perform brute-force parameter search which may be more accurate than numerical optimization. The 2P TL model is also more computationally efficient, which can be important in settings where quick decision-making is necessary. If the added complexity of the 3P TL model does not significantly improve the performance beyond a certain point, then the 2P TL model may still offer a reasonable balance between predictive performance and model simplicity.

Chapter 6: Conclusion and Future Work

Abdominal aortic aneurysm (AAA) is a serious, life-threatening condition that requires early detection and close monitoring to prevent rupture. Despite the existence of safe and reliable screening methods, like ultrasound, and programs to encourage screening, it remains a top 15 leading cause of death in the United States. In order to properly address the negative consequences of AAA on public health, more convenient, accessible, and affordable methods to detect AAA early and monitor its progression are necessary.

6.1 Limitations and Future Work

The TL model may have potential clinical value as a non-imaging solution for diagnosing and determining the success of EVAR, especially if the statistical significance of PTT between control and AAA subjects can be improved. Our work demonstrates that the TL model may be applied to aneurysmal aortas just as well as it can be applied to healthy aortas, which was previously unclear. This study also shows that PTT and wave reflection coefficient may be larger in the presence of AAA which can be explained by the theory of blood pressure wave propagation and reflection. However, there are some limitations that should be addressed in future studies to further develop TL model-enabled AAA monitoring.

For one, the differences observed in normalized PTT between control and AAA subjects were not statistically significant. Although there could be many reasons, we speculate that errors in waveform measurement or calibration and practical identifiability issues associated with the parameters may have contributed to the weakened statistical significance. This may have also affected the logistic regression's ability to effectively distinguish between control and AAA subjects. The results suggest that the efficacy of the TL model in distinguishing between control and AAA subjects is not superb, although it does exhibit adequate efficacy in distinguishing between AAA subjects before and after EVAR. This may allow TL models to be more readily applied to assess the success of EVAR.

Another limitation of this study is the lack of control for the use of medications, such as ACE inhibitors and beta-blockers, which could affect arterial stiffness and consequently, pulse transit time. This was due to incomplete drug

information for the majority of subjects in our database. In addition, comorbidities, including hypertension, hyperlipidemia, and coronary artery disease were not controlled for. As such, potential confounding effects related to medication use and comorbidities could not be accounted for, which may impact the generalizability of our findings. Future studies should aim to incorporate a more detailed assessment of medication use and comorbidities during the matching process to reduce potential confounding effects. By ensuring that these variables are accounted for, future research can more accurately isolate the effects of AAA on TL model parameters which may improve its ability to distinguish between AAA and control subjects.

The TL model still performs remarkably well considering the extreme simplicity of its structure. With more development, the TL model may play a meaningful role as a digital twin capable of personalized AAA monitoring by making it possible to measure, update, and track the model parameters on an individual basis. At the very least, the TL model parameters may complement existing AAA risk factors and biomarkers and help develop innovative approaches to ultra-convenient, accessible, and affordable non-imaging-based AAA screening and surveillance strategies. The TL model could also serve as a virtual metrology tool for personalized AAA risk assessment, integrating individual-specific data like lifestyle choices, genetic predispositions, and other risk factors to help individuals better understand and manage their risk of AAA before it becomes a problem. In this way, it can become an easily accessible “virtual advisor” to improve preventative medicine practices.

To accomplish this overarching goal and fully realize the clinical potential of TL model-enabled AAA monitoring, it may be necessary to combine the TL model with measurements that are drastically more convenient than carotid and femoral artery tonometry waveforms. For example, it would be more impactful if AAA could be monitored and managed based on (i) carotid artery tonometry and tibial artery pulse volume recording [35], (ii) brachial and tibial artery pulse volume recordings [36], or (iii) cardio-mechanical recordings like ballistocardiography, which is known to be closely associated with aortic blood pressure [47]. Future work should focus on applying the TL model to measurements available from ultra-convenient means including wearables and non-contact devices.

References

[1] S. Aggarwal, A. Qamar, V. Sharma, and A. Sharma, "Abdominal aortic aneurysm: A comprehensive review," *Exp Clin Cardiol*, vol. 16, no. 1, pp. 11–15, 2011.

[2] M. L. LeFevre and on behalf of the U.S. Preventive Services Task Force, "Screening for Abdominal Aortic Aneurysm: U.S. Preventive Services Task Force Recommendation Statement," *Ann Intern Med*, vol. 161, no. 4, pp. 281–290, Aug. 2014, doi: 10.7326/M14-1204.

[3] F. A. Lederle, "The Rise and Fall of Abdominal Aortic Aneurysm," *Circulation*, vol. 124, no. 10, pp. 1097–1099, Sep. 2011, doi: 10.1161/CIRCULATIONAHA.111.052365.

[4] J. Chung, "Epidemiology, risk factors, pathogenesis, and natural history of abdominal aortic aneurysm - UpToDate," UpToDate. Accessed: Oct. 11, 2024. [Online]. Available: https://www.uptodate.com/contents/epidemiology-risk-factors-pathogenesis-and-natural-history-of-abdominal-aortic-aneurysm

[5] L. Smith-Burgess, "Early identification and detection of abdominal aortic aneurysms," Nursing Times. Accessed: Nov. 10, 2024. [Online]. Available: https://www.nursingtimes.net/cardiovascular/early-identification-and-detection-of-abdominal-aortic-aneurysms-27-02-2017/

[6] E. J. Zucker and A. M. Prabhakar, "Abdominal aortic aneurysm screening: concepts and controversies," *Cardiovascular Diagnosis and Therapy*, vol. 8, no. Suppl 1, p. S108, Apr. 2018, doi: 10.21037/cdt.2017.09.13.

[7] E. J. Zucker, A. S. Misono, and A. M. Prabhakar, "Abdominal Aortic Aneurysm Screening Practices: Impact of the 2014 U.S. Preventive Services Task Force Recommendations," *J Am Coll Radiol*, vol. 14, no. 7, pp. 868–874, Jul. 2017, doi: 10.1016/j.jacr.2017.02.020.

[8] K. L. McGinigle, P. J. Leese, J. Trani, and L. Mureebe, "PC20. The SAAAVE Act Has Yet to Realize Its Promise in the Reduction of Ruptured Aneurysms," *Journal of Vascular Surgery*, vol. 61, no. 6, pp. 122S-123S, Jun. 2015, doi: 10.1016/j.jvs.2015.04.234.

[9] J. B. Shreibati, L. C. Baker, M. A. Hlatky, and M. W. Mell, "Impact of the Screening Abdominal Aortic Aneurysms Very Efficiently (SAAAVE) Act on abdominal ultrasonography use among Medicare beneficiaries," *Arch Intern Med*, vol. 172, no. 19, pp. 1456–1462, Oct. 2012, doi: 10.1001/archinternmed.2012.4268.

[10] G. S. Berenson, S. R. Srinivasan, W. Bao, W. P. Newman, R. E. Tracy, and W. A. Wattigney, "Association between Multiple Cardiovascular Risk Factors and Atherosclerosis in Children and Young Adults," *New England Journal of Medicine*, vol. 338, no. 23, pp. 1650–1656, Jun. 1998, doi: 10.1056/NEJM199806043382302.

[11] O. T. Raitakari *et al.*, "Cardiovascular Risk Factors in Childhood and Carotid Artery Intima-Media Thickness in Adulthood: The Cardiovascular Risk in Young Finns Study," *JAMA*, vol. 290, no. 17, pp. 2277–2283, Nov. 2003, doi: 10.1001/jama.290.17.2277.

[12] R. S. Vasan, "Biomarkers of Cardiovascular Disease," *Circulation*, vol. 113, no. 19, pp. 2335–2362, May 2006, doi: 10.1161/CIRCULATIONAHA.104.482570.

[13] K. Strimbu and J. A. Tavel, "What are Biomarkers?," *Current opinion in HIV and AIDS*, vol. 5, no. 6, p. 463, Nov. 2010, doi: 10.1097/COH.0b013e32833ed177.

[14] S. Oparil *et al.*, "Hypertension," *Nature reviews. Disease primers*, vol. 4, p. 18014, Mar. 2018, doi: 10.1038/nrdp.2018.14.

[15] M. Gao, W. C. Rose, B. Fetics, D. A. Kass, C.-H. Chen, and R. Mukkamala, "A Simple Adaptive Transfer Function for Deriving the Central Blood Pressure Waveform from a Radial Blood Pressure Waveform," *Sci Rep*, vol. 6, no. 1, p. 33230, Sep. 2016, doi: 10.1038/srep33230.

[16] G. Zhang, J.-O. Hahn, and R. Mukkamala, "Tube-Load Model Parameter Estimation for Monitoring Arterial Hemodynamics," *Front. Physiol.*, vol. 2, Nov. 2011, doi: 10.3389/fphys.2011.00072.

[17] H.-L. Kim and T. Weber, "Pulsatile Hemodynamics and Coronary Artery Disease," *Korean Circulation Journal*, vol. 51, no. 11, p. 881, Aug. 2021, doi: 10.4070/kcj.2021.0227.

[18] C. H. Chen *et al.*, "Validation of carotid artery tonometry as a means of estimating augmentation index of ascending aortic pressure," *Hypertension*, vol. 27, no. 2, pp. 168–175, Feb. 1996, doi: 10.1161/01.hyp.27.2.168.

[19] D. Gallagher, A. Adji, and M. F. O'Rourke, "Validation of the transfer function technique for generating central from peripheral upper limb pressure waveform," *American Journal of Hypertension*, vol. 17, no. 11, pp. 1059–1067, Nov. 2004, doi: 10.1016/j.amjhyper.2004.05.027.

[20] D. Moris *et al.*, "Novel Biomarkers of Abdominal Aortic Aneurysm Disease: Identifying Gaps and Dispelling Misperceptions," *BioMed Research International*, vol. 2014, p. 925840, May 2014, doi: 10.1155/2014/925840.

[21] E. Katsoulakis *et al.*, “Digital twins for health: a scoping review,” *npj Digit. Med.*, vol. 7, no. 1, pp. 1–11, Mar. 2024, doi: 10.1038/s41746-024-01073-0.

[22] M. Rashedi *et al.*, “Comparative Study on Tube-Load Modeling of Arterial Hemodynamics in Humans,” *Journal of Biomechanical Engineering*, vol. 135, no. 031005, Feb. 2013, doi: 10.1115/1.4023373.

[23] A. Mousavi, A. Tivay, B. Finegan, M. S. McMurtry, R. Mukkamala, and J.-O. Hahn, “Tapered vs. Uniform Tube-Load Modeling of Blood Pressure Wave Propagation in Human Aorta,” *Front Physiol*, vol. 10, p. 974, 2019, doi: 10.3389/fphys.2019.00974.

[24] M. Abdollahzade, C.-S. Kim, N. Fazeli, B. A. Finegan, M. Sean McMurtry, and J.-O. Hahn, “Data-driven lossy tube-load modeling of arterial tree: in-human study,” *J Biomech Eng*, vol. 136, no. 10, p. 101011, Oct. 2014, doi: 10.1115/1.4028089.

[25] Reference Values for Arterial Stiffness’ Collaboration, “Determinants of pulse wave velocity in healthy people and in the presence of cardiovascular risk factors: ‘establishing normal and reference values,’” *Eur Heart J*, vol. 31, no. 19, pp. 2338–2350, Oct. 2010, doi: 10.1093/eurheartj/ehq165.

[26] L. Jin *et al.*, “Relationship of Arterial Stiffness and Central Hemodynamics With Cardiovascular Risk In Hypertension,” *American Journal of Hypertension*, vol. 36, no. 4, pp. 201–208, Apr. 2023, doi: 10.1093/ajh/hpad005.

[27] M. K. Armstrong *et al.*, “Relation of forward and backward traveling pressure waves with subclinical carotid artery wall remodeling and central pulse pressure,” *Journal of Applied Physiology*, Oct. 2023, doi: 10.1152/japplphysiol.00286.2023.

[28] D. Kim *et al.*, “Transmission line model as a digital twin for abdominal aortic aneurysm patients,” *npj Digit. Med.*, vol. 7, no. 1, pp. 1–10, Oct. 2024, doi: 10.1038/s41746-024-01303-5.

[29] W.-C. Yu, S.-Y. Chuang, Y.-P. Lin, and C.-H. Chen, “Brachial-ankle vs carotid-femoral pulse wave velocity as a determinant of cardiovascular structure and function,” *J Hum Hypertens*, vol. 22, no. 1, pp. 24–31, Jan. 2008, doi: 10.1038/sj.jhh.1002259.

[30] C. W. Lee *et al.*, “Measures of carotid-femoral pulse wave velocity and augmentation index are not reliable in patients with abdominal aortic aneurysm,” *J Hypertens*, vol. 31, no. 9, pp. 1853–1860, Sep. 2013, doi: 10.1097/HJH.0b013e328362360a.

[31] J. Pan and W. J. Tompkins, "A Real-Time QRS Detection Algorithm," *IEEE Transactions on Biomedical Engineering*, vol. BME-32, no. 3, pp. 230–236, Mar. 1985, doi: 10.1109/TBME.1985.325532.

[32] A. Kline and Y. Luo, "PsmPy: A Package for Retrospective Cohort Matching in Python," in *2022 44th Annual International Conference of the IEEE Engineering in Medicine & Biology Society (EMBC)*, Jul. 2022, pp. 1354–1357. doi: 10.1109/EMBC48229.2022.9871333.

[33] R. Mukkamala *et al.*, "Towards Ubiquitous Blood Pressure Monitoring via Pulse Transit Time: Theory and Practice," *IEEE transactions on bio-medical engineering*, vol. 62, no. 8, p. 1879, Jun. 2015, doi: 10.1109/TBME.2015.2441951.

[34] N. Fazeli *et al.*, "Subject-specific estimation of central aortic blood pressure via system identification: preliminary in-human experimental study," *Med Biol Eng Comput*, vol. 52, no. 10, pp. 895–904, Oct. 2014, doi: 10.1007/s11517-014-1185-3.

[35] J. Lee *et al.*, "Investigation of Viscoelasticity in the Relationship Between Carotid Artery Blood Pressure and Distal Pulse Volume Waveforms," *IEEE Journal of Biomedical and Health Informatics*, vol. 22, no. 2, pp. 460–470, Mar. 2018, doi: 10.1109/JBHI.2017.2672899.

[36] Z. Ghasemi *et al.*, "Estimation of Cardiovascular Risk Predictors from Non-Invasively Measured Diametric Pulse Volume Waveforms via Multiple Measurement Information Fusion," *Sci Rep*, vol. 8, no. 1, p. 10433, Jul. 2018, doi: 10.1038/s41598-018-28604-6.

[37] M. Yavarimanesh *et al.*, "Abdominal aortic aneurysm monitoring via arterial waveform analysis: towards a convenient point-of-care device," *NPJ Digit Med*, vol. 5, no. 1, p. 168, Nov. 2022, doi: 10.1038/s41746-022-00717-3.

[38] A. Swillens *et al.*, "Effect of an abdominal aortic aneurysm on wave reflection in the aorta," *IEEE Trans Biomed Eng*, vol. 55, no. 5, pp. 1602–1611, May 2008, doi: 10.1109/TBME.2007.913994.

[39] N. P. E. Kadoglou *et al.*, "Differential effects of stent-graft fabrics on arterial stiffness in patients undergoing endovascular aneurysm repair," *J Endovasc Ther*, vol. 21, no. 6, pp. 850–858, Dec. 2014, doi: 10.1583/14-4772MR.1.

[40] N. P. E. Kadoglou *et al.*, "Changes in aortic pulse wave velocity of patients undergoing endovascular repair of abdominal aortic aneurysms," *J Endovasc Ther*, vol. 19, no. 5, pp. 661–666, Oct. 2012, doi: 10.1583/JEVT-12-3916MR.1.

[41] K. Natarajan *et al.*, “Central Blood Pressure Monitoring via a Standard Automatic Arm Cuff,” *Scientific Reports*, vol. 7, p. 14441, Oct. 2017, doi: 10.1038/s41598-017-14844-5.

[42] B. E. Westerhof *et al.*, “Arterial pressure transfer characteristics: effects of travel time,” *American Journal of Physiology-Heart and Circulatory Physiology*, vol. 292, no. 2, pp. H800–H807, Feb. 2007, doi: 10.1152/ajpheart.00443.2006.

[43] N. P. E. Kadoglou *et al.*, “Arterial stiffness and novel biomarkers in patients with abdominal aortic aneurysms,” *Regul Pept*, vol. 179, no. 1–3, pp. 50–54, Nov. 2012, doi: 10.1016/j.regpep.2012.08.014.

[44] I. Durmus, Z. Kazaz, G. Altun, and A. Cansu, “Augmentation index and aortic pulse wave velocity in patients with abdominal aortic aneurysms,” *International Journal of Clinical and Experimental Medicine*, vol. 7, no. 2, p. 421, Feb. 2014.

[45] I. Åström Malm, R. De Basso, P. Blomstrand, and N. Bjarnegård, “Increased arterial stiffness in males with abdominal aortic aneurysm,” *Clinical Physiology and Functional Imaging*, vol. 41, no. 1, pp. 68–75, 2021, doi: 10.1111/cpf.12667.

[46] X. Chen *et al.*, “Pulse Wave Velocity as a Measure of Arterial Stiffness in Patients with Abdominal Aortic Aneurysm: A Systematic Review and Meta-Analysis,” Jun. 22, 2021, *Research Square*. doi: 10.21203/rs.3.rs-615922/v1.

[47] C.-S. Kim *et al.*, “Ballistocardiogram: Mechanism and Potential for Unobtrusive Cardiovascular Health Monitoring,” *Sci Rep*, vol. 6, p. 31297, Aug. 2016, doi: 10.1038/srep31297.